

**Landslides and debris flows in the Tasman District
caused by ex-Tropical Cyclone Gita,
20-21 February, 2018**

B J Rosser

D B Townsend

J M Carey

J F Crouch

K E Jones

**GNS Science Report 2019/34
July 2020**

DISCLAIMER

The Institute of Geological and Nuclear Sciences Limited (GNS Science) and its funders give no warranties of any kind concerning the accuracy, completeness, timeliness or fitness for purpose of the contents of this report. GNS Science accepts no responsibility for any actions taken based on, or reliance placed on the contents of this report and GNS Science and its funders exclude to the full extent permitted by law liability for any loss, damage or expense, direct or indirect, and however caused, whether through negligence or otherwise, resulting from any person's or organisation's use of, or reliance on, the contents of this report.

BIBLIOGRAPHIC REFERENCE

Rosser BJ, Carey JM, Jones KE, Townsend DB, Crouch JF. 2018. Landslides and debris flows in the Tasman District caused by ex-Tropical Cyclone Gita, 20-21 February, 2018. Lower Hutt (NZ): GNS Science. 52 p. (GNS Science report; 2019/34). doi:10.21420/HN7F-K408.

B J Rosser, GNS Science, PO Box 30368, Lower Hutt, 5040, New Zealand
J M Carey, GNS Science, PO Box 30368, Lower Hutt, 5040, New Zealand
K E Jones, GNS Science, PO Box 30368, Lower Hutt, 5040, New Zealand
D B Townsend, GNS Science, PO Box 30368, Lower Hutt, 5040, New Zealand
J F Crouch, MetService, PO Box 722, Wellington 6140, New Zealand

CONTENTS

ABSTRACT	IV
KEYWORDS	IV
1.0 INTRODUCTION	1
1.1 Ex-Tropical Cyclone Gita Storm Event.....	1
1.2 Study Scope	1
1.3 Rainfall Characteristics	2
1.4 Debris Flow Terminology	6
2.0 LANDSLIDE RESPONSE.....	8
2.1 Aerial Reconnaissance Flight	8
2.2 Landslide Distribution and Types	9
2.2.1 Aorere-Kaituna River Area	9
2.2.2 Marahau-Riwaka area	13
2.3 Downstream Impacts of Debris Floods and Flows	21
3.0 LANDSLIDE SEVERITY ASSESSMENT METHODOLOGY.....	24
3.1 Data Sources.....	24
3.2 Landslide Mapping	24
3.3 Landslide Inventory Assessment Approach	27
3.4 Melton Ratios.....	28
4.0 LANDSLIDE SEVERITY ASSESSMENT RESULTS	31
4.1 Aorere-Kaituna River Area Landslides.....	32
4.2 Marahau - Riwaka Landslides.....	36
4.3 Melton Ratios.....	41
5.0 DISCUSSION.....	42
6.0 CONCLUSIONS	46
7.0 ACKNOWLEDGMENTS	48
8.0 REFERENCES	48

FIGURES

Figure 1.1	The Takaka Hill Road immediately following ex-Tropical Cyclone Gita.....	1
Figure 1.2	Rain-gauges used by MetService for the correction of rain radar data for the event.....	2
Figure 1.3	Rain radar image for the maximum 1-hour rainfall	3
Figure 1.4	Rain radar image for the 3-hour maximum rainfall total.....	4
Figure 1.5	Rain radar image for the storm total (18-hour) rainfall.....	5
Figure 1.6	Annual Return intervals for 1-hr rainfall amounts at Tasman District Council rain-gauges.....	6
Figure 2.1	Locations of photos (red dots) taken, highlighting 7 March 2018 survey flight path	8
Figure 2.2	Example of shallow debris flows sourced in soil regolith and/or colluvium overlying weathered bedrock.....	10

Figure 2.3	Damage to a bridge crossing the Kaituna River, near Aorere, caused by a channelised debris flow.....	10
Figure 2.4	Another bridge over the Kaituna River, slightly downstream from of that shown in Figure 2.3, was undermined causing the central section of the bridge to sag.	11
Figure 2.5	Examples of shallow soil and regolith landslides that occurred on open hillside faces and directly coupled to the stream channel (Upper Kaituna River).....	12
Figure 2.6	Example of landslides that occurred on open hillside faces that were directly coupled to the stream channel.....	12
Figure 2.7	Shallow debris flows initiated in soil or colluvium in gully heads in the Otuwhero River catchment.....	13
Figure 2.8	Shallow debris flows initiated in soil or colluvium in gully heads in the Atua Stream catchment, near Kaiteriteri.	14
Figure 2.9	Shallow debris flows initiated in soil or colluvium in gully heads.....	14
Figure 2.10	Shallow debris flows initiated in soil or colluvium in gully heads.....	15
Figure 2.11	Shallow debris flows initiated in soil or colluvium in gully heads in the Brooklyn Stream catchment, near Brooklyn.....	15
Figure 2.12	Shallow debris flows initiated in soil or colluvium in gully heads in the Waiwhero Creek catchment, near Pangatotara	16
Figure 2.13	Channelised debris flow on the west bank of the Motueka river, near Pangatotara.	16
Figure 2.14	Debris flow that overwhelmed the channel of a tributary to Little Pokororo River, near Ngatimoti.	17
Figure 2.15	Multiple coalesced landslides adjacent to the Marahau River that did not produce significant debris flow runoff.	17
Figure 2.16	Landslides and debris flows badly damaged the Takaka Hill Road on the north side of the Riwaka valley	18
Figure 2.17	A debris flow on the Takaka Hill Road that eroded the edge of the roadway and caused a large washout.....	18
Figure 2.18	Example of a deeper-seated landslide adjacent to an unnamed stream in the Otuwhero River catchment, near Marahau.....	19
Figure 2.19	Examples of deeper-seated landslides in the Holyoake Stream catchment, Moss Rd, near Otuwhero Inlet.....	19
Figure 2.20	Localised cracking and slumping associated with a deep-seated landslide off Little Sydney Rd, near Riwaka.	20
Figure 2.21	Localised rock falls in the Little Pokororo River catchment near Ngatimoti.	20
Figure 2.22	The locations of catchments that experienced debris flows during ex-Tropical Cyclone Gita.....	21
Figure 2.23	Debris flow deposit in the Otuwhero River near the upper end of the floodplain.	22
Figure 2.24	Debris flow deposit in the Otuwhero River catchment, at Otuwhero Valley Rd.	22
Figure 2.25	Thin debris flow and over bank deposits, lower Holyoake Stream valley and mouth, Otuwhero inlet.....	23
Figure 3.1	Sentinel-2 10 m True Colour Image tiles captured on A-B) 24 January 2018 and C-D) 23 February 2018, following ex-Tropical Cyclone Gita	25
Figure 3.2	Red band change detection methodology for extracting landslide polygons	26
Figure 3.3	Mapped landslide (pink) and overbank deposition (green) polygons in the Otuwhero catchment using the Red Band Automatic extraction method from 10 m Sentinel imagery	27
Figure 3.4	Location of the 58 catchments used to calculate Melton Ratios for this study.....	30
Figure 4.1	Location of landslides and debris flood/flow deposits triggered by ex-Tropical Cyclone Gita, showing the two areas of landslides.....	31

Figure 4.2	Landslide source areas shown in relation to the underlying geology (after Heron 2018) in the Aorere-Kaituna area.	33
Figure 4.3	Landslide source areas shown in relation to Land use categories from LCDB 2012.	34
Figure 4.4	The location of landslide source areas shown in relation to the storm rainfall total	36
Figure 4.5	Relationship between landslide density and storm rainfall.	37
Figure 4.6	Landslide source area locations shown in relation to the underlying geology (after Heron 2018). Separation Point Granite is highlighted in green.	38
Figure 4.7	The distribution of landslides triggered by ex-Tropical Cyclone Gita in relation to main vegetation and land use classes (as mapped in 2012) in the Marahau-Riwaka area.	39
Figure 5.1	Aerial photographs of landslides in The Shaggery catchment taken a) before (2016) and b) after ex-Tropical Cyclone Gita	44

TABLES

Table 1.1	Maximum rainfall totals (gauge-corrected, in mm) for different time periods for ex-Tropical Cyclone Gita, recorded at the Wellington radar (Data provided by MetService).....	3
Table 4.1	Frequency of landslides (LS) triggered in different geological units in the Aorere-Kaituna area.	35
Table 4.2	The frequency of landslides occurring in each of the Land use categories from LCDB2 2012.	35
Table 4.3	The frequency of landslides occurring in each of the slope categories.	35
Table 4.4	Percentage (by number) of landslides (LS) triggered in each of the main geological units in the Marahau-Riwaka area.	40
Table 4.5	The frequency of landslides occurring in each of the slope categories.	40
Table 4.6	The frequency of landslides occurring in the main land use categories	40
Figure 4.8	Melton Ratio and catchment length for the 58 affected catchments in the Marahau area	41
Table 5.1	Previous storm events that have triggered debris flows in the Tasman District.....	43

APPENDICES

APPENDIX 1	CATCHMENT CHARACTERISTICS AND MELTON RATIOS	51
-------------------	--	-----------

ABSTRACT

Ex-Tropical Cyclone Gita hit New Zealand on 20–21 February 2018, bringing heavy rain and high winds to much of the country. The heaviest rainfall occurred in the Tasman District where more than 230 mm of rain fell in 18 hours triggering extensive shallow landslides and debris flows. The Takaka Hill Road was closed by 16 slips, which impacted the road for the following year. The most intense rainfall (78 mm/hr) occurred over a 3-hour period between 3 pm and 6 pm near Marahau and it was during this period that most of the landslides were triggered. Annual recurrence intervals (ARI) for the rainfall in this area may have exceeded 200 years, however the heaviest rainfall was isolated and for most rain gauges the ARI was <10 years.

An aerial reconnaissance was flown by GNS Science and Tasman District Council staff on 7 March 2018. A regional-scale assessment was undertaken to map the landslides triggered by ex-Tropical Cyclone Gita by differencing of the pre- and post-event, 10-m resolution Sentinel satellite imagery. The extreme rainfall triggered more than 2000 landslides, in two distinct areas: 1) Aorere-Kaituna River area, near Collingwood (417 landslides) and 2) Marahau-Riwaka area northwest of Motueka (1638 landslides). The highest density of landsliding occurred along the northern end of the Arthur Range (Takaka Hill). Debris flows were initiated in several of the receiving catchments, particularly in the Riwaka-Marahau area, where significant debris flows occurred in the Otuwhero, Marahau, Riwaka, Rocky and the Shaggery rivers. The landslide distribution was overlaid onto attribute layers containing key site characteristics (rainfall, geology, slope angle, slope aspect, vegetation type) to assess their potential controlling influence. Melton ratios, a measure of the ability of catchments to generate debris flows that has been used to identify debris flow prone catchments, were calculated for each catchment in the area of heaviest rainfall. The distribution of landslides was strongly influenced by the underlying geology, with 80 % of the landslides occurring on Separation Point Granite which underlies only 23 % of the area where landslides occurred. Rocks of the Separation Point Granite suite are often deeply weathered and highly erodible. The rainfall threshold for triggering debris flows in Separation Point Granite was about 200 mm/18 hrs, or 120 mm/3 hrs. This equates to rainfall intensities >10 mm/hr for longer durations (18 hrs) or 40 mm/hr for short durations (<3 hrs).

Analysis of the landslide distribution in relation to the rainfall estimates derived from rain radar identified several key issues with the rain radar data, mostly associated with the distance of the site from the Wellington radar station. Firstly, because of the distance from the radar station to the site, the rainfall was measured at an altitude of 3-4 km. With northerly winds of 110-130 km/hr, it was estimated that the rain fell on the ground roughly 10 km south of where it was measured in the air. Secondly, the radar had difficulty 'seeing through' the heavy rain at Abel Tasman National Park and underestimated the rainfall in the Aorere-Kaituna River area. Ideally, when using rain radar to investigate rainfall induced landslides, it should be corrected to the local rain-gauge network, corrected for wind, and used with caution.

KEYWORDS

Cyclone Gita, debris flow, rain radar, Separation Point Granite, Melton Ratio, rainfall induced landslide; Tasman District

1.0 INTRODUCTION

1.1 Ex-Tropical Cyclone Gita Storm Event

Ex-Tropical Cyclone Gita impacted New Zealand on 20 and 21 February 2018 bringing heavy rain and high winds to most regions. The heavy rain was experienced over much of the country and triggered many landslides (<https://www.geonet.org.nz/news/2ghEz2MkiOIQKqIOkyw42I>). The Tasman District experienced the heaviest rainfall during the storm, with a local State of Emergency being declared for the District, after more than 200 mm of rain fell between 7 am and 6 pm on Tuesday 20th February. Extensive shallow landslides and debris flows were triggered in the Riwaka – Marahau area. The Takaka Hill Road was closed by 16 slips (Figure 1.1), isolating about 6000 people (including residents and tourists) in Golden Bay, with the road closed for 2 weeks while NZTA reinstated it. Impacts are ongoing with engineering works on some of the larger landslides expected to be completed in 2020 or later. There were also debris flows reported in the Aorere and Kaituna River catchments in the Kahurangi National Park. State Highway 60, from Riwaka to Takaka, was also temporarily closed due to fallen trees, slips and flooding. There was localised flooding in Motueka, Takaka and Marahau, and the Riwaka River burst its banks causing significant flooding on the Riwaka Plains.

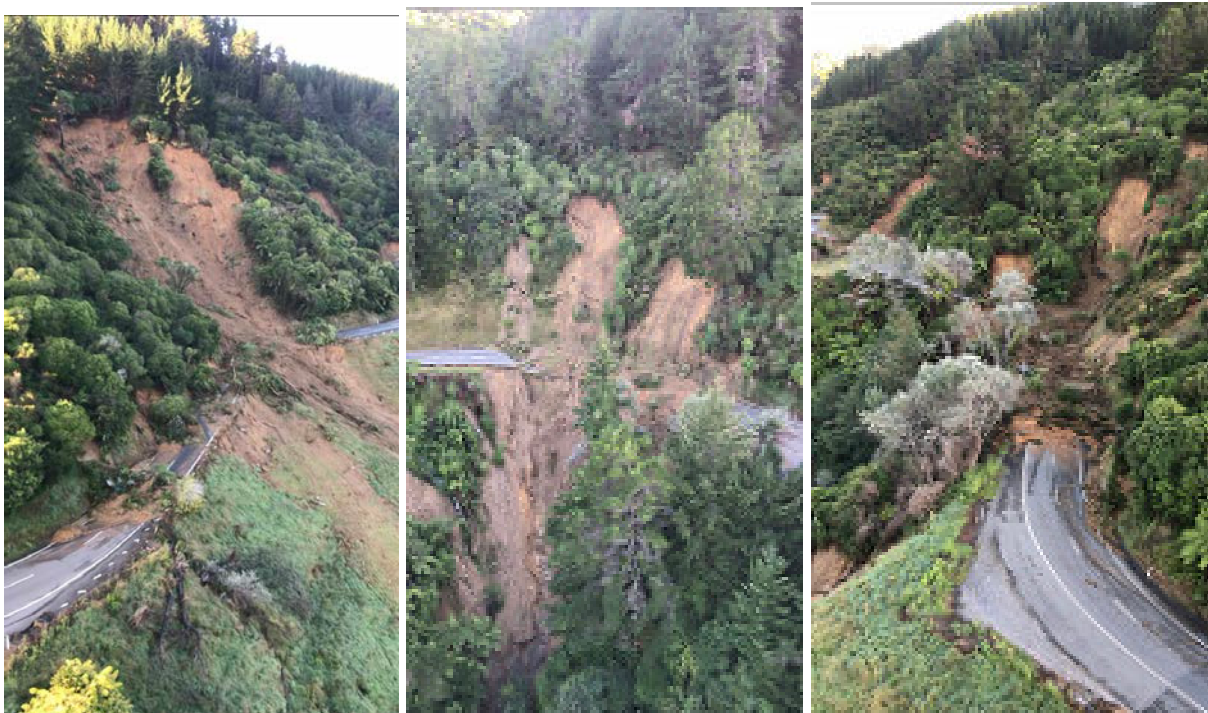


Figure 1.1 The Takaka Hill Road immediately following ex-Tropical Cyclone Gita (Photos: NZTA, 22 February 2018).

1.2 Study Scope

A Geonet landslide response was undertaken after the storm to record the nature, extent and impact of landsliding across the two worst affected regions; the Tasman and Kaikoura regions. Given the distances between the two regions the responses were conducted and reported on separately.

This report provides the findings of the Tasman Geonet response and specifically aims to identify the size, number, distribution and impacts of landslides that occurred across the region and their relationship to key site characteristics including rainfall, geology, and land use.

1.3 Rainfall Characteristics

Tasman District Council rain gauges recorded the heaviest rainfall between 4 am and 10 pm on February 20th, 2018 (New Zealand daylight-savings time - NZDT). Up to 235 mm of rain fell over the area north of Marahau, about 195 mm at Marahau, and about 175-190 mm fell on the eastern part of the Takaka Hill with the maximum rainfall (235 mm) recorded at Riwaka (Tasman District Council).

Rain radar data was recorded approximately 140 km from Marahau at Wellington. MetService provided gauge-corrected rain radar data for the event. The rain radar correction was made using a combination of available MetService, Tasman and Marlborough District Council and HortResearch rain gauges, shown in Figure 1.2. Gauge-corrected rain radar totals for the maximum 1-hour, 3-hour, 6-hour, 12-hour and 18-hour (storm total) for this event for various locations are summarised in Table 1.1 and the maximum 1-hour, 3-hour and 18-hour (storm total) rainfall totals are illustrated in Figure 1.3 to Figure 1.5.

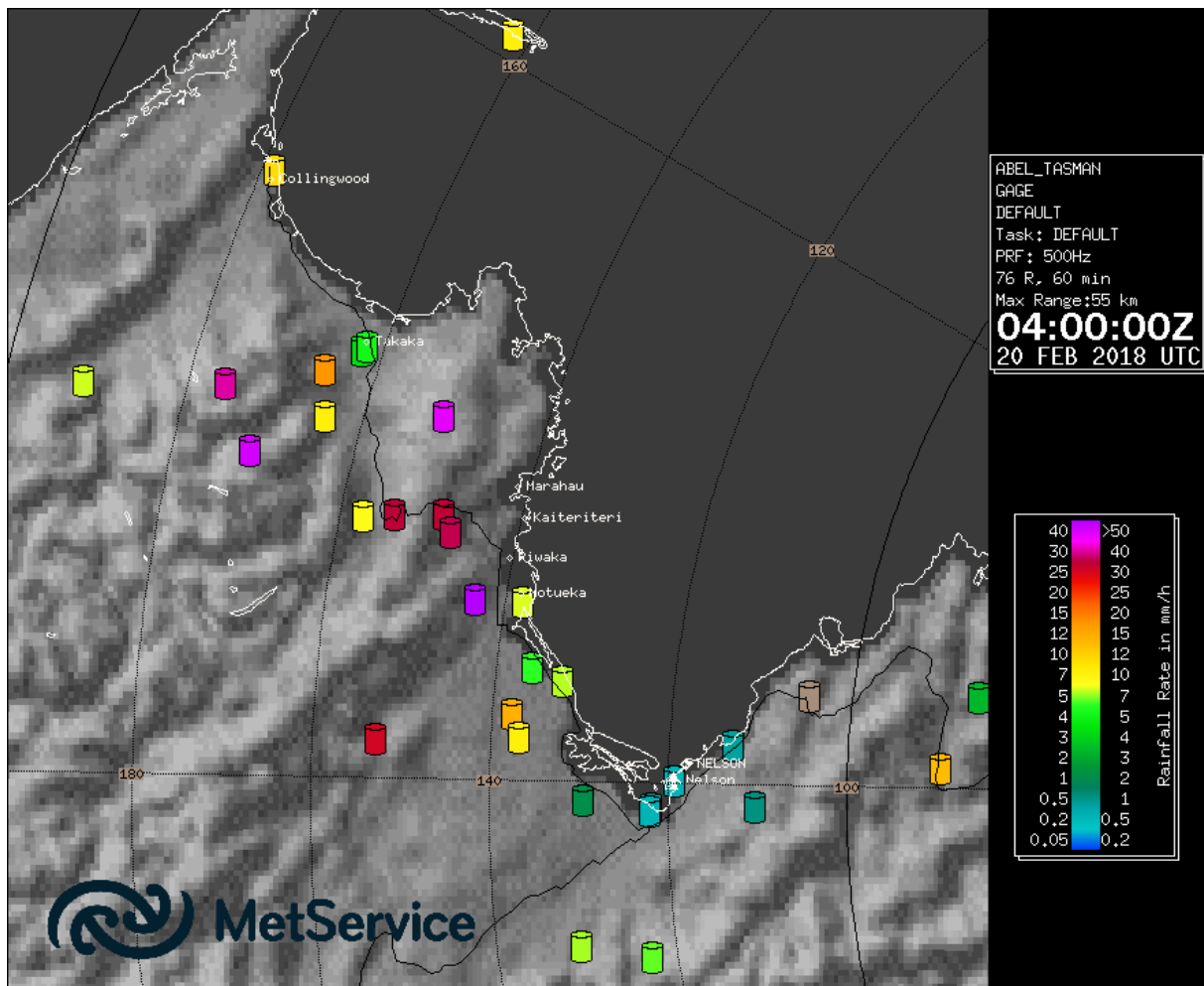


Figure 1.2 Rain-gauges used by MetService for the correction of rain radar data for the event. Map shows the 1-hour rainfall intensity in mm/hr during the period of heaviest rain between 03 and 04 UTC (4 pm and 5 pm NZDT) 20 February 2018.

Table 1.1 Maximum rainfall totals (gauge-corrected, in mm) for different time periods for ex-Tropical Cyclone Gita, recorded at the Wellington radar (Data provided by MetService).

Location	Rainfall measurement period				
	1 hr	3 hrs	6 hrs	12 hrs	18 hrs*
North of Marahau	78	148	180	220	235
Marahau	70	120	150	185	195
Riwaka	55	90	125	170	190

*storm event total

The radar data demonstrates that the most intense rainfall was isolated and occurred over a 3-hour period between 3 pm and 6 pm (NZDT) in the Riwaka and Marahau areas (Figure 1.4). It was during this 3-hour period that most of the landslides were triggered (Glenn Stevens, pers comm). These areas had already received approximately 80 mm over the preceding 12 hours.

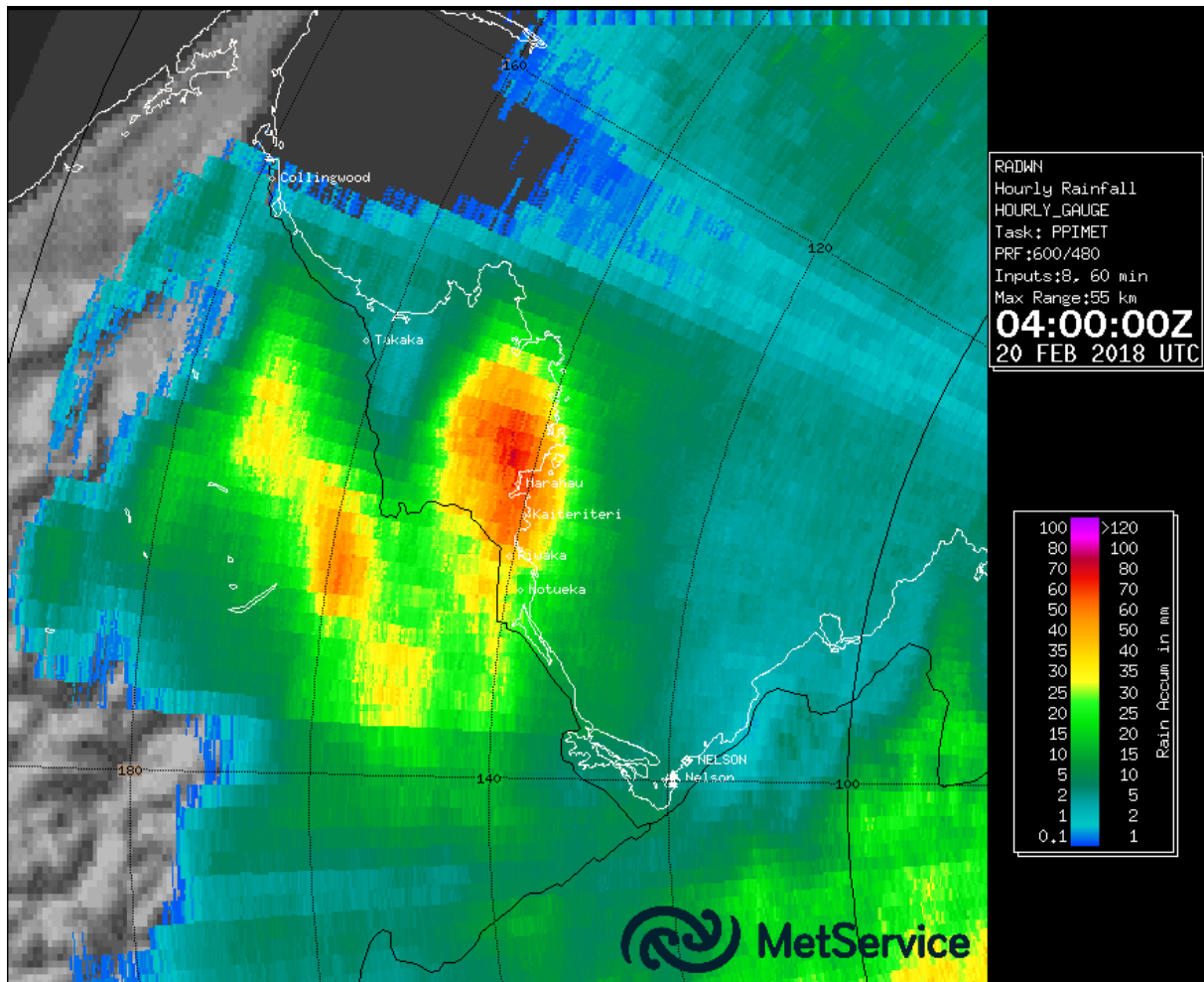


Figure 1.3 Rain radar image for the maximum 1-hour rainfall. The maximum 1-hour rainfall occurred in the area north of Marahau and over the Takaka Hill between 03 and 04 UTC 20/02/2018 (4-5pm NZDT) and was typically between 60–75 mm/hr, with a maximum value of 78 mm/hr just to the north of Marahau.

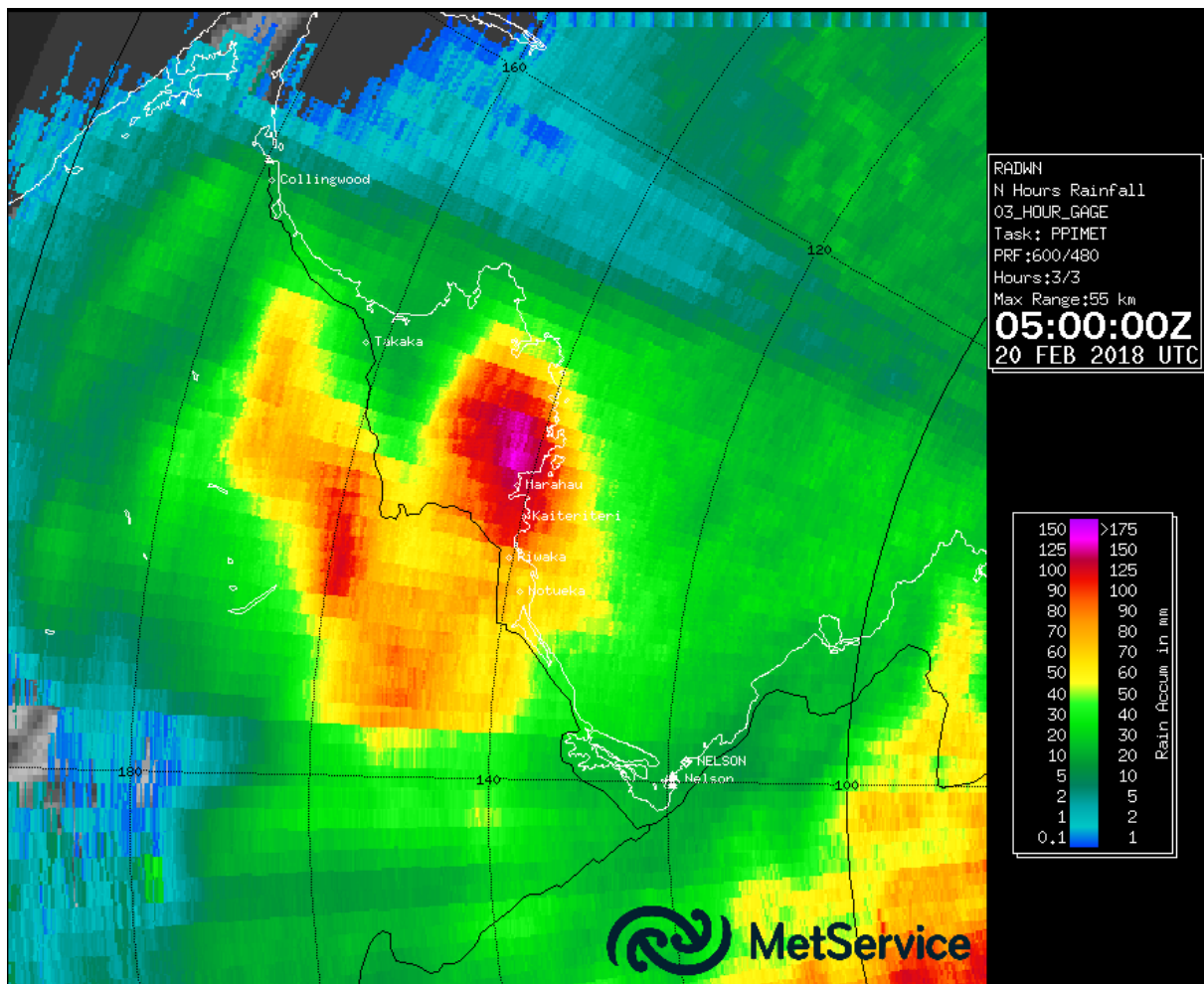


Figure 1.4 Rain radar image for the 3-hour maximum rainfall total. The 3-hour maximum rainfall occurred in the area north of Marahau between 02 and 05 UTC 20/02/2018 (3-6 pm NZDT) and was between 130–140 mm, with a maximum value of 148 mm just to the north of Marahau. This 3-hour period is when most of the landslides were triggered. (Note scale is different to Figure 1.3).

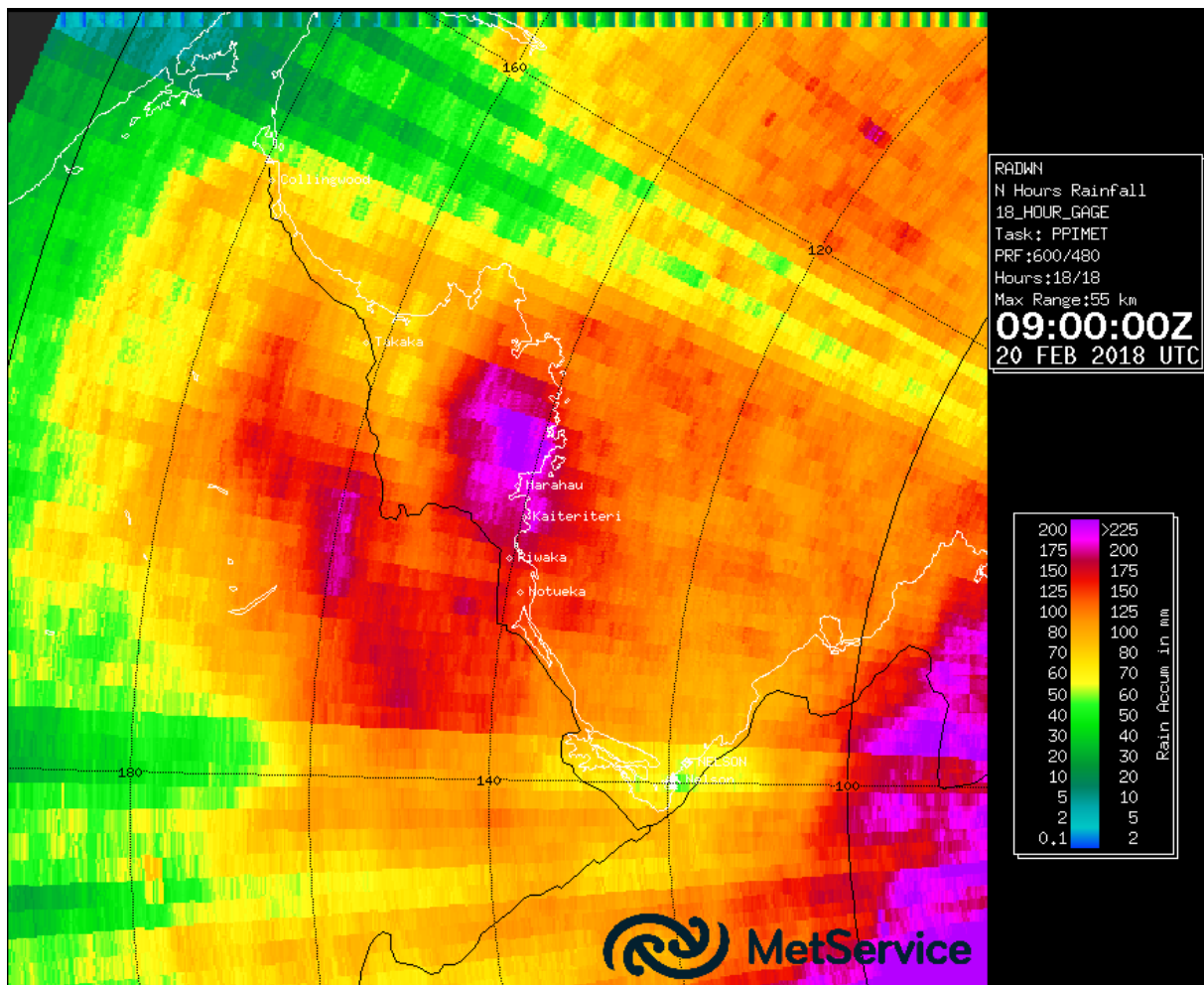


Figure 1.5 Rain radar image for the storm total (18-hour) rainfall. The maximum 18-hour rainfall occurred in the area north of Marahau from 15:00 UTC 19/02/2018 to 09:00 UTC 20/02/2018 (4am–10pm NZDT) with rainfall totals of about 230–235 mm over the area north of Marahau, about 195 mm over Marahau, and about 175–190 mm about the eastern part of the Takaka Hill Road. (Note scale is different to Figure 1.3 and Figure 1.4).

Data from the National Institute for Water and Atmospheric Research’s (NIWA) High Intensity Rainfall Design System (HIRDS) (<https://hirds.niwa.co.nz>) indicates that the annual return interval (ARI) for the 1, 12, and 18-hour rainfall totals for the areas that received the maximum amount of rain (Marahau and Riwaka) during ex-Tropical Cyclone Gita were in excess of 100 years, and the ARI for the 1 and 12-hour totals may exceed 200 years at Marahau and the Abel Tasman National Park. However, as indicated in Figure 1.6, at most rain gauges in the region, the ARI for the 1-hour maximum was below 10 years, which further demonstrates that the heaviest rainfall was very localised.



Figure 1.6 Annual Return intervals for 1-hr rainfall amounts at Tasman District Council rain-gauges (Data from Tasman District Council/HIRDS).

1.4 Debris Flow Terminology

The term ‘debris flow’ is used by natural hazard specialists to describe a particular type of mass flow which is a rapidly moving, extremely mobile mixture of water and sediment. However, to the general public, especially those who have experienced debris flows, these are often referred to as ‘floods’ or ‘flash floods’ because of the speed at which they travel, both within a stream channel and also once they overflow onto a fan surface. The behaviour and composition of a debris flow is very different from that of a conventional flood. Debris flows only occur under specific catchment and rainfall conditions and involve a number of different processes. They are generally restricted to small, steep catchments where slope sediment and channel sediment are plentiful. For the same amount of rain, a debris flow has a much higher discharge than a flood, it contains more and often larger rock debris, and it moves faster. As a consequence, debris flows are usually more destructive and dangerous than floods.

A debris flow usually commences in a short, steep stream when a landslide or a number of landslides are initiated during a period of intense (or prolonged) rainfall. These initiating slides are often small (only a few tens of cubic metres in volume), but they may coalesce to form larger debris flows or avalanches. If the debris enters a steep, confined channel, its volume may increase as it moves rapidly downstream due to scouring and entrainment of sediment stored in the bed and along the banks of the stream. A debris flow can also be caused by the blockage of a channel, often by a landslide or woody debris, and initiated when the trapped water is suddenly released by failure of the dam. A debris flow commonly moves in distinct surges or slugs of debris, separated by watery inter-surge flows. A debris flow event may consist of one surge or many tens of surges.

Such surges are characterised by boulder fronts (boulders and other large (woody) debris) and lateral levees. The debris flow typically deposits sediment to form a colluvial/debris fan at the base of the steep catchment where the slope reduces, and the stream becomes unconfined. The coarsest debris is deposited near the head of the fan, so that towards the distal end of the fan, sediment concentration, particle size and flow velocity have reduced, and the process is then referred to as a debris flood. Debris floods are not as damaging as debris flows as they do not carry such large debris. Because the larger boulders are deposited at the head of the fan, successive pulses of debris flows are readily diverted by this material, making the flow path unpredictable.

The technical definitions of the various terms used in this report are taken from Hungr et al. (2005, 2014):

- A debris avalanche is a very rapid to extremely rapid (5–20 m/s, 15–60 km/hr), shallow slide or flow of partially or fully water-saturated debris on a steep slope, which is not confined within an established channel.
- A debris flow is a very rapid to extremely rapid (5–10 m/s, 15–30 km/hr) flow of water-saturated, non-plastic (granular) debris in a steep channel. Speeds are often faster than a fit human can run. The sediment has a consistency of wet concrete, with sediment concentrations often in excess of 60 % by volume (80 % by weight) compared to flood waters, where sediment concentrations are generally <4 % by volume (10 % by weight).
- A debris flood is a very rapid (up to ~5 m/s), surging flow of water, heavily charged with debris, in a steep channel. A debris flood almost always occurs as a continuation downstream of a debris flow but can occur in the absence of a debris flow.

The term debris flow is also used to describe the entire phenomenon from initiating landslide on a steep slope, the rapid flow along a confined channel, and the deposition on a debris fan (Hungr et al. 2005, 2014). There is almost always a debris flood as a continuation downstream of a debris flow, and it is usual to extend the term debris flow to include the associated debris flood when referring to the entire event. It should be noted that a debris flood can occur in the absence of a debris flow. When a debris flood occurs without an associated debris flow, the distinction between the two is usually easiest made on the basis of peak discharge during an event. Peak discharge during a debris flood is limited to at most 2–3 times that of a major flood as it results in relatively low flow depths. Peak discharges from a debris flow can be as much as 50 times as large as those of a major flood. Their destructive potential therefore, is much greater than that of a flood.

2.0 LANDSLIDE RESPONSE

2.1 Aerial Reconnaissance Flight

An aerial reconnaissance was flown by helicopter on Wednesday 7th March 2018 including Dougal Townsend and Jon Carey (GNS Science), and Glen Stevens (Tasman District Council). The flight took approximately 2 hours between 12 pm and 2 pm, initially in clear, sunny weather conditions, but which became cloudy farther west. The flight path focussed on areas where landslides had been reported (Figure 2.1).

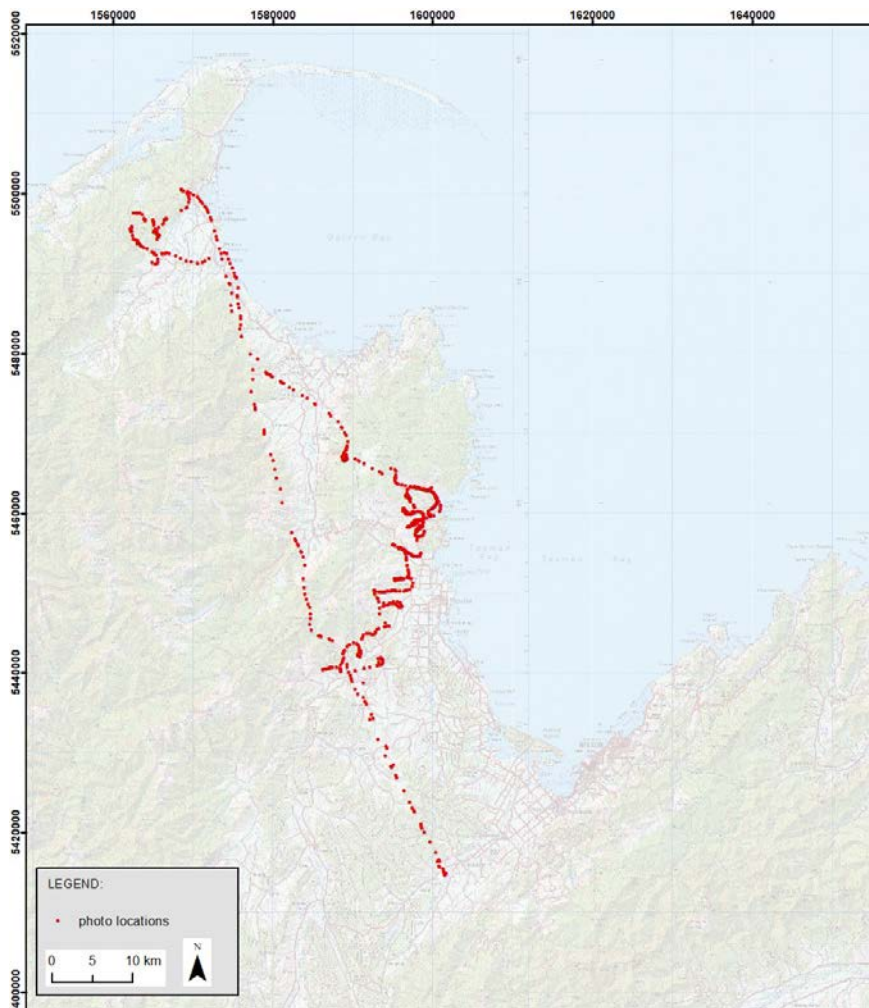


Figure 2.1 Locations of photos (red dots) taken, highlighting 7 March 2018 survey flight path. Note: not all photos are of landslides.

2.2 Landslide Distribution and Types

Landslides triggered by ex-Tropical Cyclone Gita were concentrated in two main areas:

1. Aorere-Kaituna River area, c. 10 km west of Collingwood described in section 2.2.1, and
2. Marahau-Riwaka area and other river catchments to the north west of Motueka described in section 2.2.2.

2.2.1 Aorere-Kaituna River Area

A cluster of landslides was observed in the Aorere-Kaituna River area in the Kahurangi National Park, and along the SE-facing side of the Burnett Range to the north (Figure 2.1). The landslides were predominantly shallow debris flows, sourced in soil regolith and/or colluvium overlying weathered bedrock, mainly initiating in heads of gullies (Figure 2.2). The majority of debris flows were strongly coupled with stream channels, which confined debris flow runout along the channel networks. In some locations, the debris flows were able to spread over flatter, farmed terrain lower in the catchments. A concentrated debris flow caused notable damage to a bridge (Figure 2.3) crossing the Kaituna River. In this location, water and entrained debris (mainly trees) were built up behind the bridge before spilling out onto the surrounding farm land. Another bridge further downstream was undermined and had supporting material washed away from the foundations of its central pile, causing the central section of the bridge to sag (Figure 2.4).

In addition to debris flows in gully heads, several landslides occurred on open hillside faces (Figure 2.5 and Figure 2.6). While these landslides were also typically shallow failures in soil regolith and colluvium overlying weathered bedrock (and in some instances ran out to reach the stream channels), they appeared to have occurred less frequently than the channelised debris flows.



Figure 2.2 Example of shallow debris flows sourced in soil regolith and/or colluvium overlying weathered bedrock. Tributary of Granity Creek, Aorere River. There is also an older landslide scar on the hillslope on the right-hand side.



Figure 2.3 Damage to a bridge crossing the Kaituna River, near Aorere, caused by a channelised debris flow. In this location water and entrained debris (mainly trees) built up behind the bridge before spilling out onto the surrounding farm land.



Figure 2.4 Another bridge over the Kaituna River, slightly downstream from of that shown in Figure 2.3, was undermined causing the central section of the bridge to sag.



Figure 2.5 Examples of shallow soil and regolith landslides that occurred on open hillside faces and directly coupled to the stream channel (Upper Kaituna River).



Figure 2.6 Example of landslides that occurred on open hillside faces that were directly coupled to the stream channel (Kaituna River, near Mt Hardinger).

2.2.2 Marahau-Riwaka area

Most of the high density landsliding occurred within the southeast facing sub-catchments of the Motueka River, along the northern end of the Arthur Range (Takaka Hill), about 8 km west of Motueka. As also observed in the Aorere-Kaituna area, the predominant landslide type was shallow debris flow (Figure 2.7). Again, these were mainly initiated in gully heads in soil regolith and/or colluvial deposits (Figure 2.8 and Figure 2.9) overlying weathered bedrock. Whilst the majority initiated in natural ground (Figure 2.10), several debris flows initiated from forestry roads or skid platforms (Figure 2.11 and Figure 2.12). Most of the debris flows were strongly coupled to channels and so were mainly confined (Figure 2.13), or they coalesced and spread out when reaching flatter terrain (Figure 2.14). Not all cases of coalescing landslides into a channel produced a debris flow (Figure 2.15).

Debris flows that initiated above the Takaka Hill Road on the north side of the Riwaka valley inundated the road, making it impassable; some of these flows had enough power to erode the edge of the roadway, causing wash-outs below the road (Figure 2.16 and Figure 2.17).

In addition, several deeper-seated landslides and flows were observed (Figure 2.18 and Figure 2.19), some of which also involved local cracking and slumping (Figure 2.20). Some localised rock falls were also identified (Figure 2.21).



Figure 2.7 Shallow debris flows initiated in soil or colluvium in gully heads in the Otuwhero River catchment.



Figure 2.8 Shallow debris flows initiated in soil or colluvium in gully heads in the Atua Stream catchment, near Kaiteriteri.



Figure 2.9 Shallow debris flows initiated in soil or colluvium in gully heads. Several debris flows initiated from forestry roads or skid platforms (far centre) (tributary of Holyoake Stream, near Kaiteriteri).



Figure 2.10 Shallow debris flows initiated in soil or colluvium in gully heads (tributary of Holyoake Stream, near Kaiterteri).



Figure 2.11 Shallow debris flows initiated in soil or colluvium in gully heads in the Brooklyn Stream catchment, near Brooklyn. Several debris flows initiated from forestry roads or skid platforms.



Figure 2.12 Shallow debris flows initiated in soil or colluvium in gully heads in the Waiwhero Creek catchment, near Pangatotara. Several debris flows initiated from forestry roads or skid platforms.



Figure 2.13 Channelised debris flow on the west bank of the Motueka river, near Pangatotara.



Figure 2.14 Debris flow that overwhelmed the channel of a tributary to Little Pokororo River, near Ngatimoti.



Figure 2.15 Multiple coalesced landslides adjacent to the Marahau River that did not produce significant debris flow runout.



Figure 2.16 Landslides and debris flows badly damaged the Takaka Hill Road on the north side of the Riwaka valley. In some instances, the road was inundated by debris making it impassable. Many of the debris flows had enough power to erode the edge of the roadway, causing wash-outs below the road.



Figure 2.17 A debris flow on the Takaka Hill Road that eroded the edge of the roadway and caused a large washout (Photo: Stuff.co.nz, 22 February 2018).



Figure 2.18 Example of a deeper-seated landslide adjacent to an unnamed stream in the Otuwhero River catchment, near Marahau.



Figure 2.19 Examples of deeper-seated landslides in the Holyoake Stream catchment, Moss Rd, near Otuwhero Inlet.

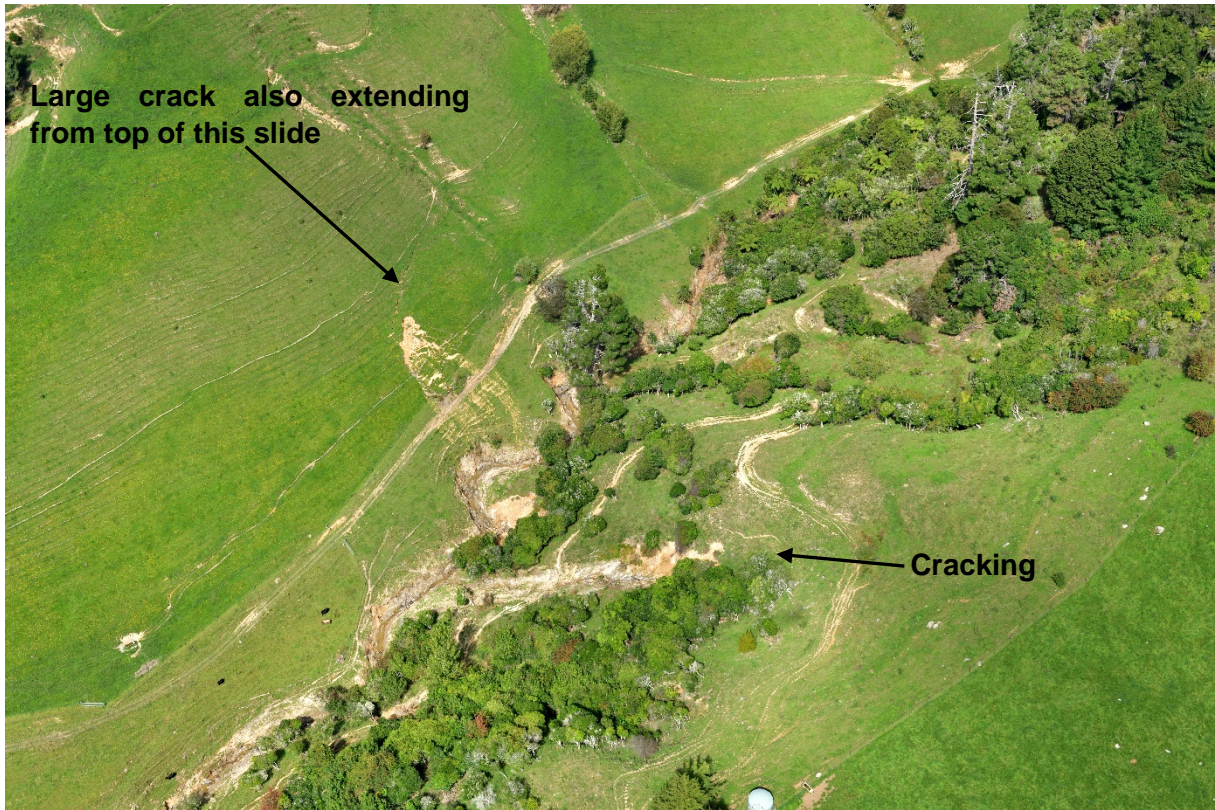


Figure 2.20 Localised cracking and slumping associated with a deep-seated landslide off Little Sydney Rd, near Riwaka.

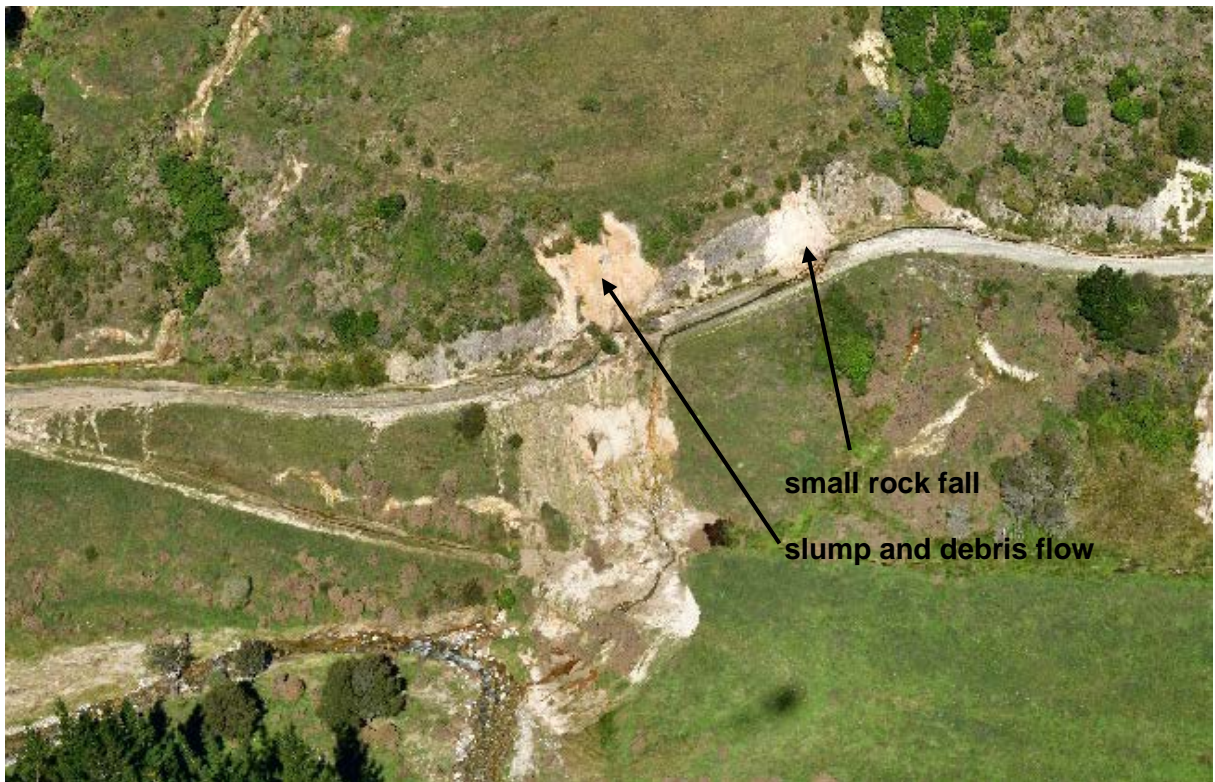


Figure 2.21 Localised rock falls in the Little Pokororo River catchment near Ngatimoti.

2.3 Downstream Impacts of Debris Floods and Flows

Debris floods and flows occurred in many of the river and stream channels downstream of the landslides. The locations of these catchments are shown in Figure 2.22. The catchments where debris flows occurred in the Riwaka-Marahau area included the Marahau River, Otuwhero River (Figure 2.23 and Figure 2.24), Holyoake Stream (Figure 2.25), Riwaka River and lower sub catchments of the Motueka River including Brooklyn Stream, the Shaggery, and Rocky River. In the Kahurangi National Park area, debris floods and/or flows occurred in at least 6 sub-catchments of the lower Aorere and Kaituna Rivers.



Figure 2.22 The locations of catchments that experienced debris flows during ex-Tropical Cyclone Gita.



Figure 2.23 Debris flow deposit in the Otuwhero River near the upper end of the floodplain.



Figure 2.24 Debris flow deposit in the Otuwhero River catchment, at Otuwhero Valley Rd.



Figure 2.25 Thin debris flow and over bank deposits, lower Holyoake Stream valley and mouth, Otuwhero inlet.

3.0 LANDSLIDE SEVERITY ASSESSMENT METHODOLOGY

3.1 Data Sources

A rapid, regional-scale assessment was undertaken of landslide severity by comparing before and after storm satellite imagery to identify and map new landslides. Sentinel-2 Level-1C data was downloaded from the ESA Sentinel data hub (<https://scihub.copernicus.eu>), and images with minimal cloud cover capturing immediate post-event damage were selected (Figure 3.1). 23 February 2018 was chosen as the closest post-event image Level-1C data, which is processed by ESA, includes radiometric and geometric corrections (Top-Of-Atmospheric reflectance and orthorectification) and is tiled into 100 km x 100 km in UTM WGS84 projection. Only the 10 m bands, including visible Red, Green, Blue (RGB) and Near-Infrared (NIR), were used for further analysis. The pre- and post-event tiles were imported into ArcMap and checked for geometry accuracy against baseline topographic data as an RGB True Colour Image (TCI) built from band 02 (Blue), band 03 (Green) and band 04 (Red).

3.2 Landslide Mapping

Landslide polygons were extracted using a semi-automated approach by identifying pixels with a visual change when the pre- and post-event images were compared. An automated extraction of likely landslide scars as polygon features in a GIS environment was then used to rapidly determine potential landslide locations (Figure 3.2). Given that fresh landslide scars, debris tails, and the presence of fine sediment on the floodplain appears bright and highly reflective when viewing the TCI, we used strong spectral difference between the pre- and post-event landslide imagery to indicate recent landslide scars and run-out debris. By calculating the change in the pixel value across a single band (B04 Red), and extracting the pixels with highest variance, a polygon set representing the landslide (source area plus debris trail), and overbank deposition was generated (Figure 3.3).

To improve accuracy, the processing window was confined to areas with observed fresh landslides following ex-Tropical Cyclone Gita. Some landslides were observed outside this processing window, but these features could be identified in the 24 January 2018 images, indicating that they were not generated by this storm. This dataset was manually checked and false positives (e.g. cloud cover) were removed, and each polygon was attributed as either landslide scar (source area plus debris tail) or debris (overbank deposition). The result was two sets of fresh bare ground polygons with a minimum area of 100 m², representing the change between 24 January 2018 and 23 February 2018.

Detailed interrogation of the landslide distribution indicated that misclassifications of landslide source areas had occurred in some areas (Figure 3.4). Given the scale of the satellite imagery (10x10 m minimum pixel size) it was not possible to differentiate between deposition in headwater channels and landslides, or bank erosion adjacent to the stream channel. This was rectified where possible but it is acknowledged that the number of landslides may be overestimated as a consequence of this. It was also not possible to differentiate between landslide source areas and deposits, so the landslide polygons represent landslide scar (source) plus deposit combined. Due to the scale of the satellite imagery it is also likely that smaller landslides (100–300 m²) were not detected, which included but was not limited to new landslides in close proximity to existing landslides, and enlargement or reactivation of existing landslides.

Catchments where debris floods and flows occurred were also identified. No fieldwork was undertaken so it was not possible to differentiate between debris floods and flows. The area of deposition was mapped from satellite imagery using the method described above. Catchment polygons (River Environment Classification) were downloaded from Land Information New Zealand (LINZ) and the area of each catchment was calculated. It was noted whether a debris flood/flow occurred within that catchment. Landslide densities were then calculated for each of the catchments.

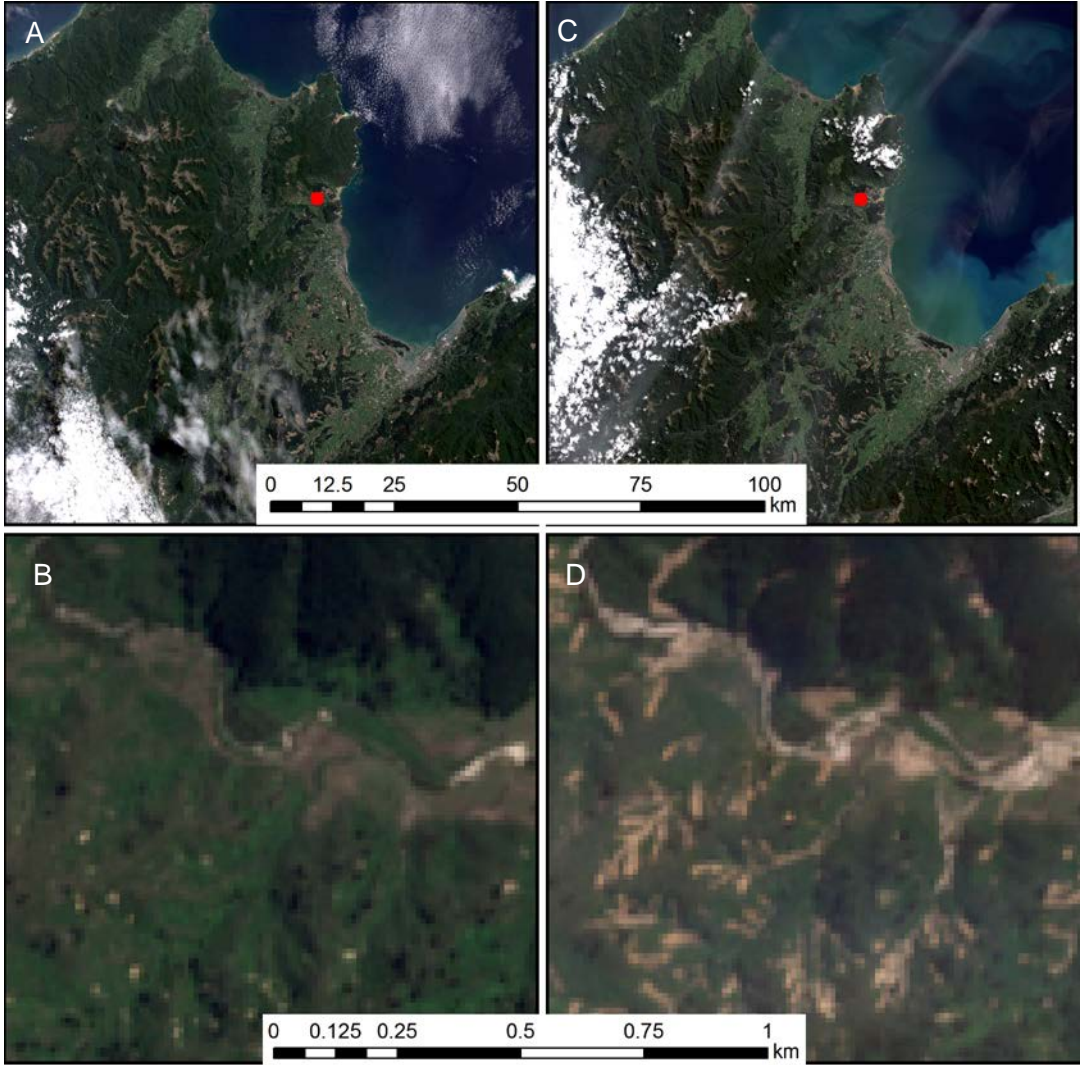


Figure 3.1 Sentinel-2 10 m True Colour Image tiles captured on A-B) 24 January 2018 and C-D) 23 February 2018, following ex-Tropical Cyclone Gita. Landslide damage in the Riwaka area (red square) is clearly visible on C-D. (Copernicus Sentinel data 2018, processed by ESA).

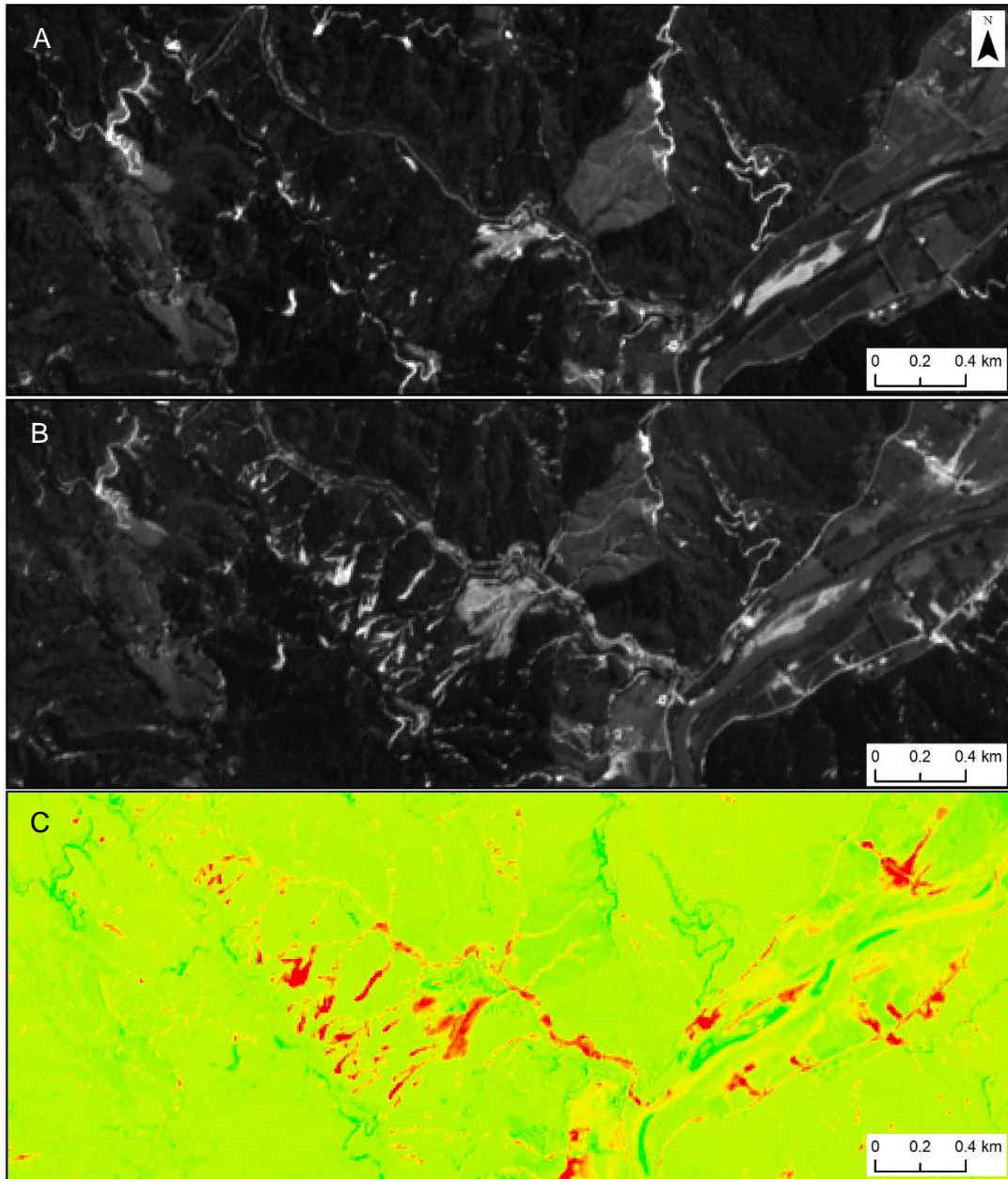


Figure 3.2 Red band change detection methodology for extracting landslide polygons A) Sentinel-2 pre-event dataset showing only the red band stretch. B) Sentinel-2 post-event dataset showing only the red band stretch; the landslide scars can be seen (in white) with high red band pixel values. C) Difference between the pre- and post- red band datasets, showing areas with a significant increase in red band values as red. These areas show stronger reflection due to the bright, fresh landslide scars and sediment transported downslope.

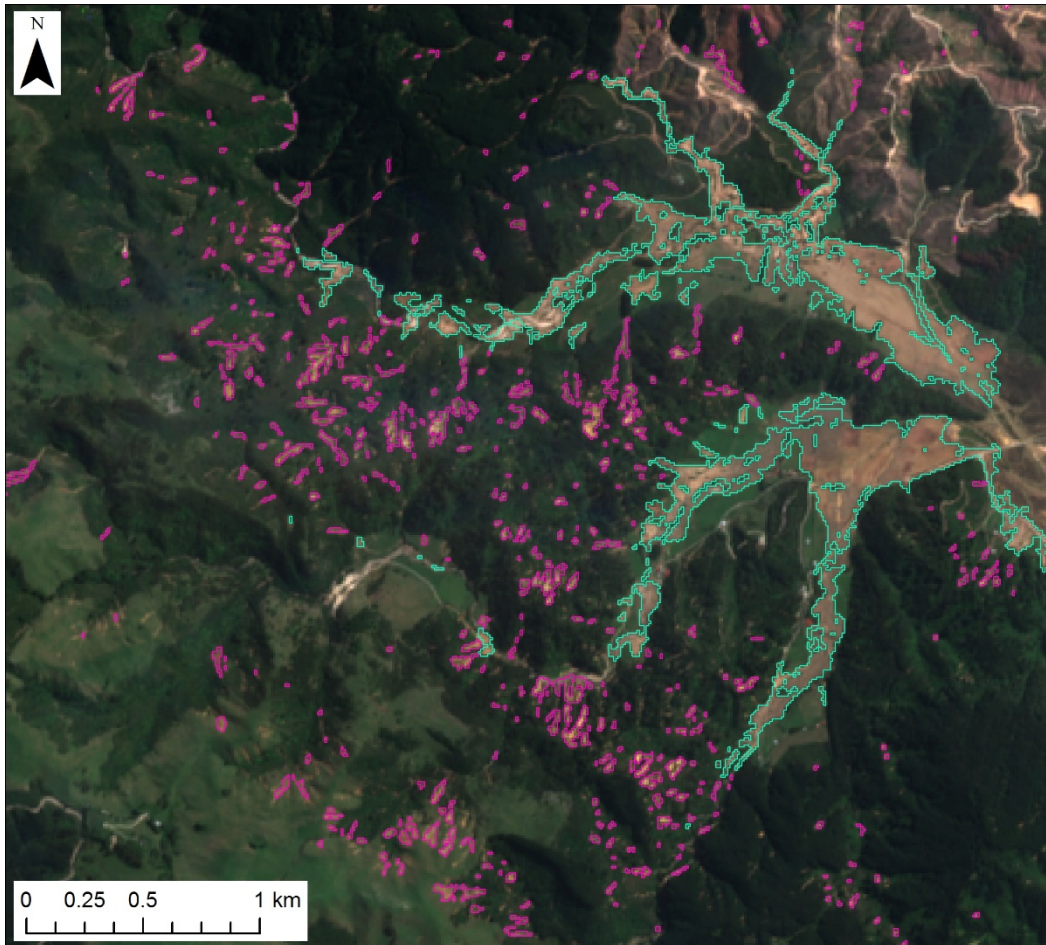


Figure 3.3 Mapped landslide (pink) and overbank deposition (green) polygons in the Otuwhero catchment using the Red Band Automatic extraction method from 10 m Sentinel imagery. Background image 23 February 2018 (Copernicus Sentinel data 2018, processed by ESA).

3.3 Landslide Inventory Assessment Approach

The landslide polygons derived from satellite imagery differencing were overlaid with attribute layers containing key site characteristics in ArcGIS to assess their potential influence in controlling the observed landslide distribution. Zonal statistics were extracted for each landslide source area and were categorised by the site characteristics that covered more than 50 % of the landslide source area (areas <50 % were ignored). The site characteristics used comprised:

- **Rainfall:** The 1 hr max (maximum intensity), 18 hr maximum rainfall (storm total) and the mean rainfall values were extracted from the rain radar data for each landslide source area. The rain radar data was contoured into 10 mm contour intervals (isohyets), and the area covered by each interval was calculated. A landslide density (landslides/km²) was then calculated for each rainfall contour.

- **Geology:** The 1: 250 000 regional geological map (after Heron 2018 – QMAP seamless data) was used to determine the geological materials of each landslide source area. The units were simplified and were grouped into 6 main geological units:
 - Separation Point Granite
 - Mount Arthur Group (marble, schist)
 - Riwaka Igneous Complex (diorite, gabbro)
 - Moutere Gravel (Tadmor Group)
 - Pleistocene alluvium
 - Holocene alluvium (river and fan deposits)
- **Slope angle:** An 8 m resolution digital elevation model (DEM) from LINZ was used to develop a series of slope angle classes based on Hancox et al. (2002) to determine the slope angle at each landslide source area.
- **Vegetation / land use:** Vegetation and land use classes from the Land Cover Data Base version 2) (LCDB2), as mapped in 2012 at 1:50 000 scale, were grouped into the following categories:
 - Indigenous forest (includes Broadleaved Indigenous Hardwoods, Indigenous Forest)
 - Scrub (includes Fernland, Gorse and/or Broom, Manuka and/or Kanuka)
 - Exotic Forest
 - Forest – Harvested
 - Pasture (includes High Producing Exotic Grassland, Low Producing Grassland)
 - Other (includes Deciduous Hardwoods, Orchard, Vineyard or Other Perennial Crop, Transport Infrastructure, Built-up Area)
- **Slope aspect:** An 8 m resolution DEM from LINZ was used to calculate the mean slope aspect for each landslide source area. Slope aspects were categorised into 15-degree bins, and the number of landslides in each category was calculated.

3.4 Melton Ratios

The debris flow hazard in the Tasman District was first identified as a concern when the May 2010 Tapawera and December 2011 Golden Bay storms triggered debris flows that caused considerable damage to structures built on fans (Basher 2010, Page et al. 2012). Page et al. (2012) calculated Melton Ratios, an index of catchment ruggedness, to identify catchments capable of generating debris flows. See Welsh and Davies (2010) and Page et al. (2012) for further discussion about the use of Melton Ratios for identifying debris flow-prone catchments. It must be emphasised that this approach provided a preliminary assessment of potential debris flow-prone catchments and fans, and any fans on which development is proposed require thorough site investigations. The Melton Ratio (R) is equal to catchment relief divided by the square root of catchment area:

$$R = H_b / \sqrt{A_b}$$

where H_b is catchment relief and A_b is catchment area. Catchments with a Melton Ratio >0.5 are capable of generating debris flows. Welsh and Davies (2010) applied the Melton Ratio to 18 catchments in the Coromandel and Kaimai Ranges, 16 catchments in the Southern Alps and 2 catchments at Matata, all known to have generated debris flows in the past. They found

that all catchments had a Melton Ratio > 0.5 except those at Matata. Catchments with a Melton Ratio >0.3 were capable of producing debris floods, and those where the Melton Ratio was <0.3 were dominated by fluvial processes.

Page et al. (2012) concluded that Melton Ratios, in combination with catchment length, could be used to identify debris flow-prone catchments, but that the thresholds may be different for different terrains/landscapes, and that the thresholds for debris flow triggering on Separation Point Granite require refinement with further data. The debris flows generated by ex-Tropical Cyclone Gita in the Marahau-Riwaka area provided the opportunity to add to the debris flow data for catchments underlain by Separation Point Granite. No field work was undertaken as part of this project, so it was not possible to differentiate between debris flows and debris floods (see above).

There were 58 catchments identified between the Pokororo River (Graham Valley Rd) in the south to the Marahau River in Abel Tasman National Park in the north, that received the most rainfall during ex-Tropical Cyclone Gita. All comprise steep hillslopes underlain by Separation Point Granite. The size of the catchment contributing area (upstream of the fan apex) ranges from 0.4 to 26.3 km², and the catchment lengths (upstream of the fan apex) range from 0.8 to 9.5 km. Land cover included exotic forest, indigenous forest and scrub. The areas of exotic forest include areas of recently harvested forest and young pine plantings (<6 yrs old).

The 58 catchments were delineated in ArcGIS using the 8 m DEM from LINZ and were categorised according to whether or not a debris flood or flow occurred using the post-event 0.3 m orthorectified colour aerial photography provided by TDC (Figure 3.4). The aerial photography was not used to produce the landslide distribution due to time and resource constraints. Catchment length was calculated as the planimetric distance from the apex of the fan to the furthest point on the catchment boundary, the catchment area was calculated as the area that drains to the apex of the fan (referred to as contributing catchment area), and catchment relief (altitude range) was calculated from the 8 m DEM.

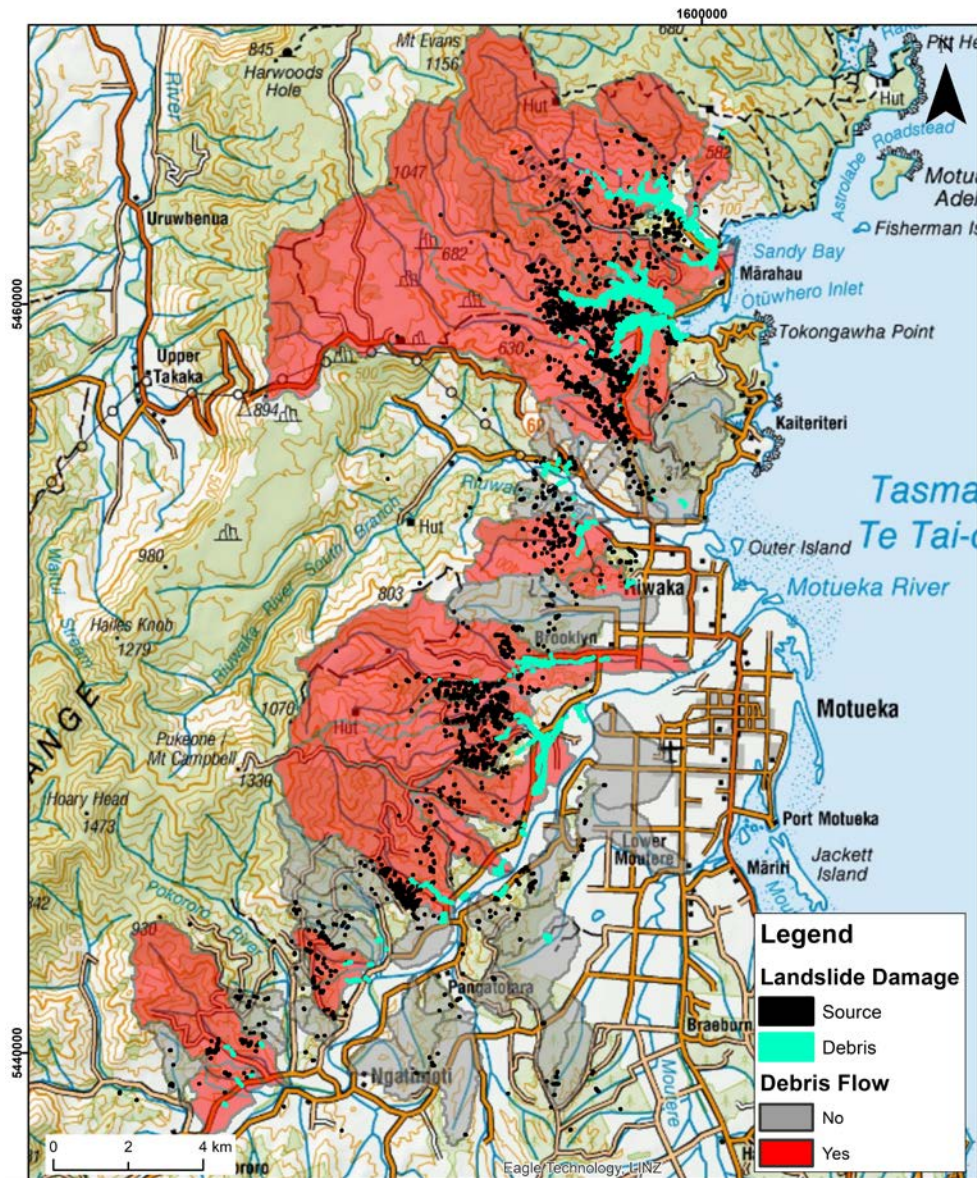


Figure 3.4 Location of the 58 catchments used to calculate Melton Ratios for this study. The catchments that generated a debris flood or flow are shown in red, and those that didn't in grey.

4.0 LANDSLIDE SEVERITY ASSESSMENT RESULTS

Our analysis identified 1958 landslides across the study area that were triggered during ex-Tropical Cyclone Gita (Figure 3.4). The landslides occurred in two distinct areas. The majority (1638) of the landslides occurred along south-east facing hill range north west of the Motueka valley, from Ngatimoti in the south to Marahau in the north. The remaining 417 landslides occurred along the south-east facing Burnett Range in the Aorere-Kaituna River area in the Kahurangi National Park, c. 10 km west of Collingwood. These two areas are a significant distance (50 km) apart with distinctively different geology and topography and are therefore discussed separately in sections 4.1. and 4.2 below.

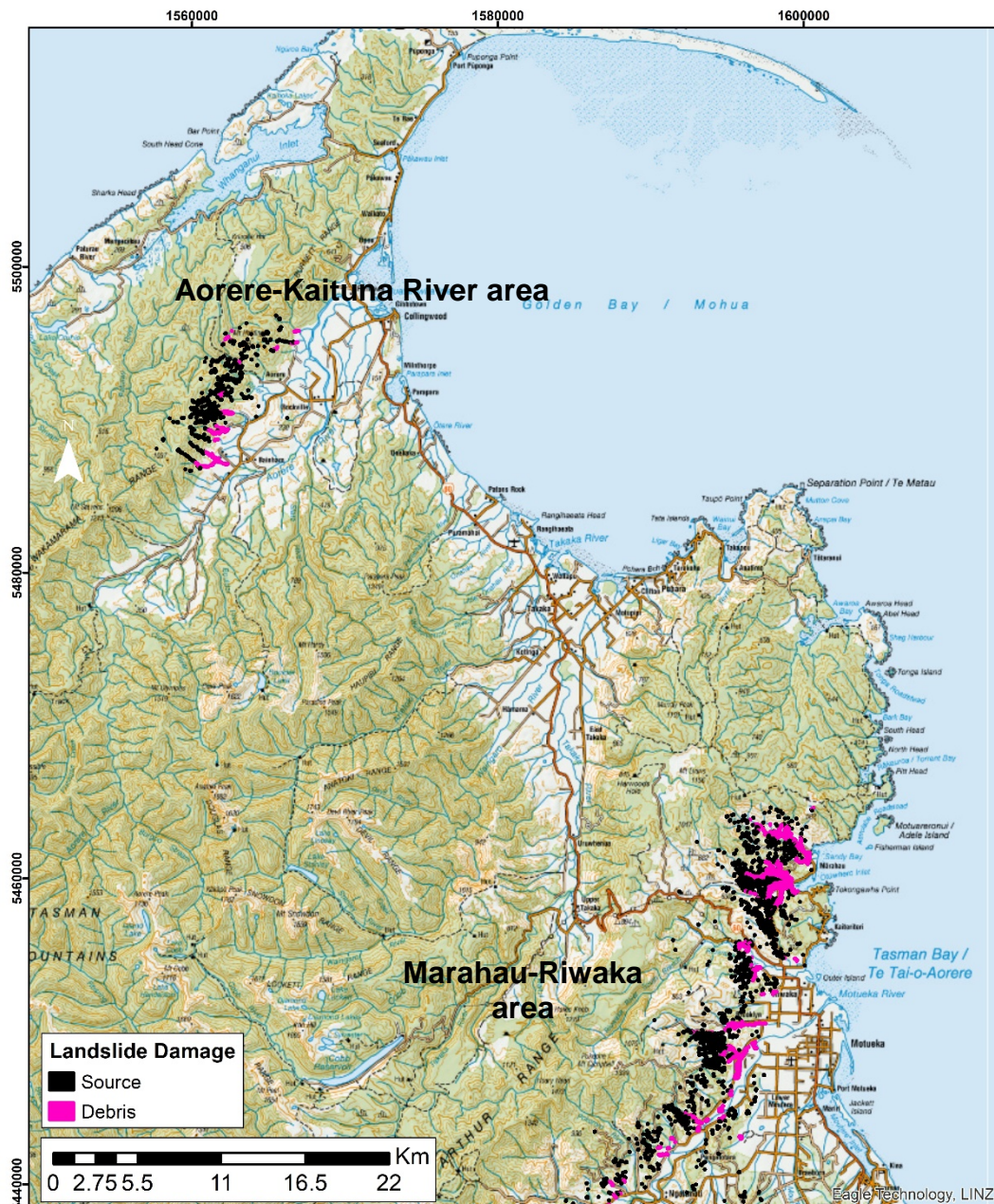


Figure 4.1 Location of landslides and debris flood/flow deposits triggered by ex-Tropical Cyclone Gita, showing the two areas of landslides.

4.1 Aorere-Kaituna River Area Landslides

The satellite differencing identified 417 landslides over an area of 38 km² of the Aorere-Kaituna River area of the Kahurangi National Park. These mostly occurred along the SE-facing side of the Burnett Range (**Error! Reference source not found.**) with a maximum density of 11 landslides/km². The average landslide size (source + deposit) was 1089 m².

In the Aorere-Kaituna River area, rainfall statistics, extracted for each landslide source area from the rain radar, estimate a rainfall minimum of 50 mm and maximum of 87 mm over the 18-hour period. A maximum hourly intensity of 6.4 mm/hr was recorded for the event in this area. Given that the area has a vegetation cover of indigenous forest, it is unlikely that landslides would have been triggered by such low rainfall. The locally operated TDC 'Aorere at Devils Boot' rain gauge recorded 60.4 mm between 2 pm and 5 pm on 20 February, with hourly intensities ranging from 17.3 to 22.9 mm/hr during this period. This was not picked up by the rain radar (Figure 1.3) and was not used for the gauge correction. A further MetService rain gauge at Farewell Spit recorded 110.4 mm over 24 hours (no hourly data available) which also does not seem to be picked up by the rain radar. In both instances, such rainfall conditions would be expected to trigger landslides (Rosser et al. 2020 in review).

The geology in the affected area includes Cambrian breccia and schistose rocks in the Kaituna valley and Cretaceous conglomerate capping the steep hills to the north (Rattenbury et al. 1998). The landslides were triggered over a range of rock types as summarised in Table 4.1 and illustrated in Figure 4.2. The majority of failures (73 %) were underlain by two geological units which occupy approximately 50 % of the study area. These are sandstones of the Anatoki Formation (42%) and the Waingaro greenschist (31%).

The vegetation in this area is dominantly indigenous forest cover, which may have been selectively logged in the past. The main vegetation and land use classes (as mapped in 2012) in the Aorere-Kaituna River area is shown in Figure 4.3. The frequency of landslides occurring in each of the land use categories is shown in Table 4.2. Of the landslides triggered by ex-Tropical Cyclone Gita in the Aorere-Kaituna area, 92 % occurred on slopes with Indigenous forest cover, which is not surprising given that this makes up 82 % of the affected area.

Although the majority of landslides occurred on slopes with indigenous forest cover, the area of highest landslide density classified by the semi-automated method occurred on 'other' land uses, which were all existing landslides (there were 5). This indicates that several existing landslides were reactivated.

Most landslides occurred on slopes with angles between 25 and 35 degrees (Table 4.3). Landslides predominantly occurred on north-east facing slopes, with 72 % of landslides occurring on slopes with aspect between 030 and 150 degrees (NNE to SE).

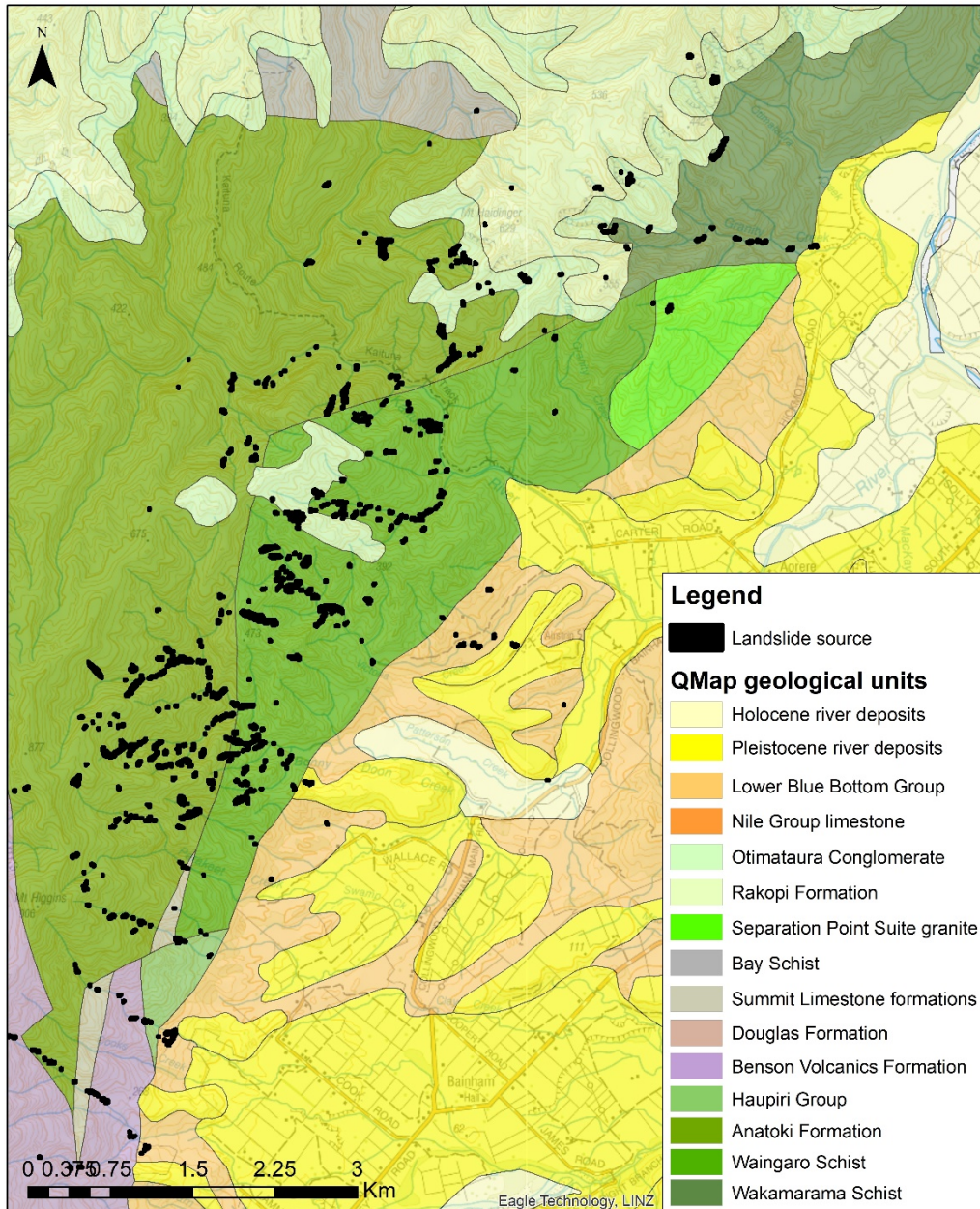


Figure 4.2 Landslide source areas shown in relation to the underlying geology (after Heron 2018) in the Aorere-Kaituna area.

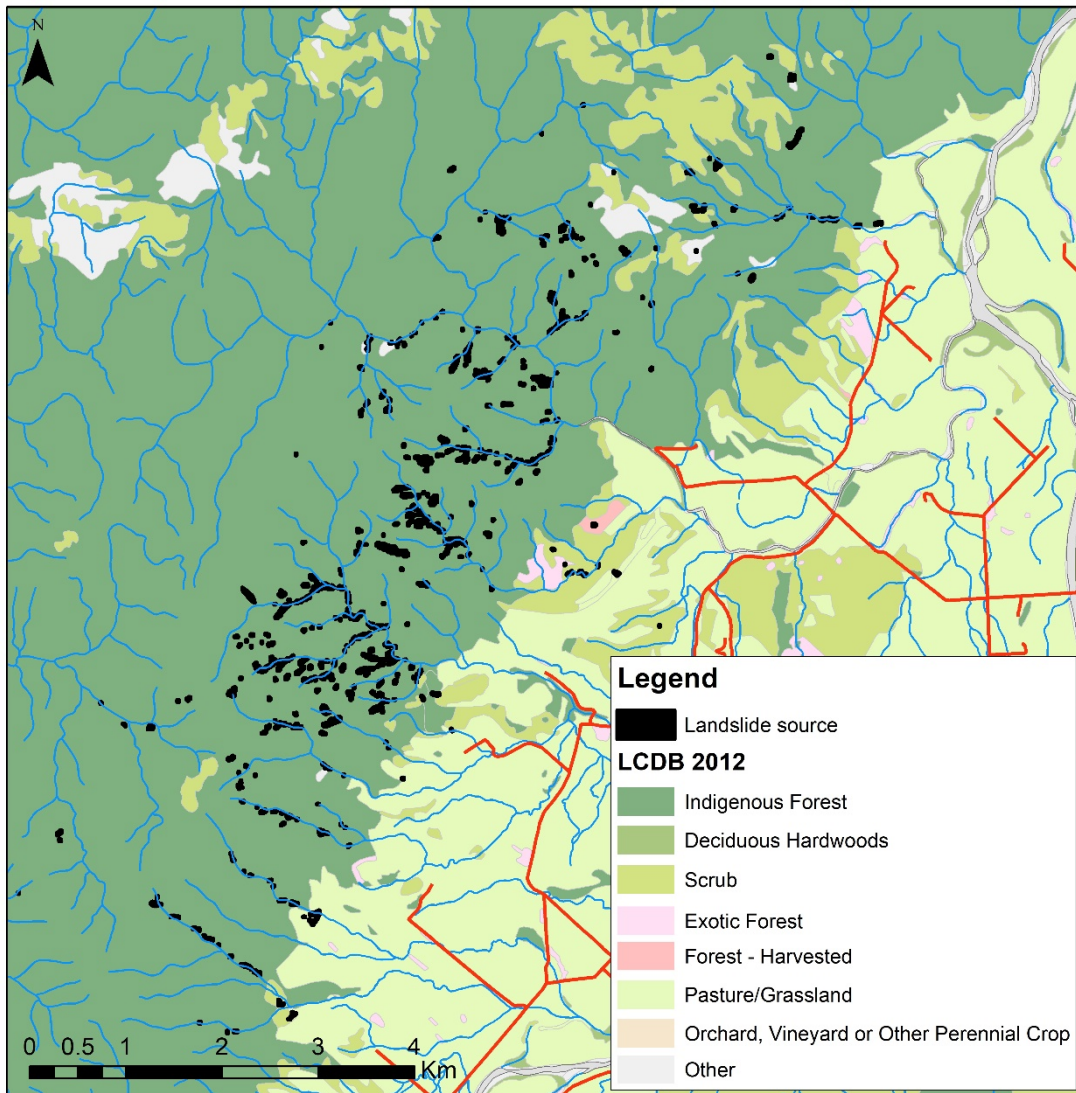


Figure 4.3 Landslide source areas shown in relation to Land use categories from LCDB 2012.

Table 4.1 Frequency of landslides (LS) triggered in different geological units in the Aorere-Kaituna area.

Geological Unit	Main rock type	Number	%	% of affected area	LS/km ²
Anatoki Formation	sandstone	175	42.0	29.5	5.9
Bay Schist	schist	1	0.2	0.4	2.8
Benson Volcanics Formation	basalt	22	5.3	11.1	2.0
Douglas Formation	argillite	1	0.2	0.1	1.0
Haupiri Group	siltstone	6	1.4	1.1	7.4
Lower Blue Bottom Subgroup	siltstone	19	4.6	8.5	2.2
Otimataura Conglomerate	conglomerate	23	5.5	6.6	3.5
Rakopi Formation	sandstone	8	1.9	6.3	1.3
Separation Point Granite	granite	5	1.2	3.7	1.3
Summit Limestone	limestone	4	1.0	1.0	4.2
Waingaro Schist	greenschist	139	31.3	21.9	6.4
Wakamarama Schist	schist	10	2.4	4.7	2.1
Other		2	0.5	5.2	0.4
Total		417	100	100	

Table 4.2 The frequency of landslides occurring in each of the Land use categories from LCDB2 2012.

Land use category (LCDB2)	Number	%	% of affected area	LS/km ²
Scrub	17	4.1	8.7	5.2
Indigenous forest	382	91.6	81.7	12.4
Exotic Forest	1	0.2	0.5	4.9
Forest - Harvested	1	0.2	0.2	14.1
Pasture	11	2.6	7.8	3.8
Other	5	1.2	1.0	13.0
Total	417	100	100	

Table 4.3 The frequency of landslides occurring in each of the slope categories.

Slope category	Number	%	% of affected area	LS/km ²
<25	103	24.8	21.7	11.9
25-35	130	31.2	22.4	15.0
35-45	136	32.8	29.8	11.8
45-60	47	11.2	24.1	5.1
>60	0	0.0	1.3	0
Total	417	100	100	

4.2 Marahau - Riwaka Landslides

Satellite imagery differencing mapped 1638 landslides in the Marahau-Riwaka region, over an area of about 130 km² (density of 12.6 landslides/km²). This area received the highest rainfall during the storm event (up to 235 mm over 18 hours) and landslides were initiated on slopes on slopes between 25 and 35 degrees. The average landslide size (source + deposit) was 783 m². This area is mainly underlain by Cretaceous Separation Point Granite and is covered by a variety of vegetation types including native forest, regenerating forest/scrub, exotic forestry and cleared farmland.

The maximum rainfall of 235 mm over the 18-hour duration of the storm was recorded in the Abel Tasman National Park, to the north of Marahau (Figure 1.5). The maximum rainfall intensity of 75 mm/hr was also recorded in this area (Figure 1.3), and up to 175 mm of rain fell in just 3 hours (Figure 1.4). The average rainfall intensity for the storm was 13 mm/hr. The landslide distribution is shown in relation to the storm rainfall total in Figure 4.4. The threshold for landsliding in the storm event in the Marahau area was about 60 mm/3 hrs or 130mm/18 hrs.

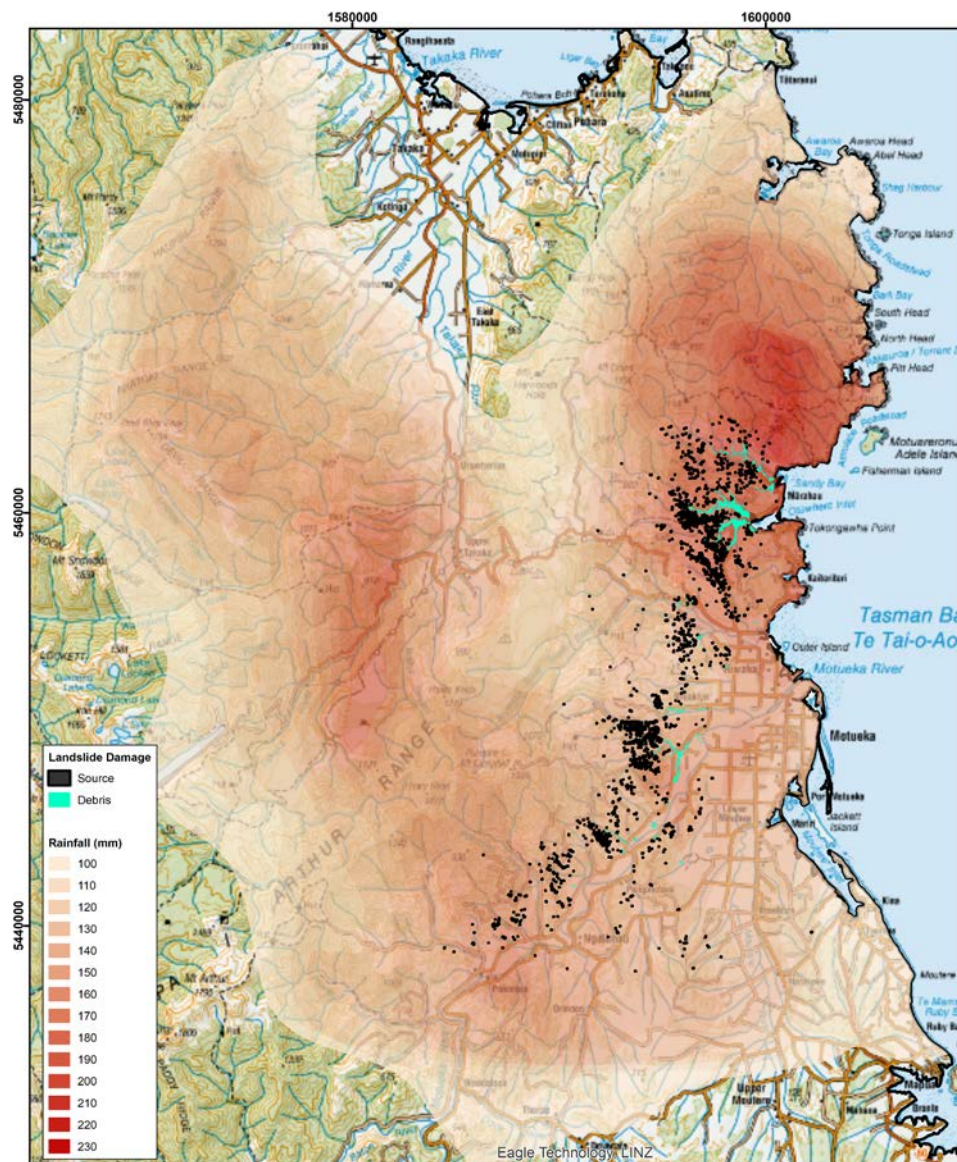


Figure 4.4 The location of landslide source areas shown in relation to the storm rainfall total (over 18 hrs). Rainfall contour intervals calculated from the rain radar statistics are also shown for the area of >100 mm rainfall.

Although there is an increasing number (and density) of landslides as rainfall increased, there was not a simple relationship between rainfall amount and landslide density (Figure 4.5). The data indicates that the maximum landslide density occurred in the areas that received 190–200 mm of rainfall, not in the area that received the maximum rainfall (235 mm/18 hrs). The northern limit of landslides is the Marahau River catchment, although the highest rainfall was just north of this area. The northern extent of the landslides was confirmed using the TDC aerial photography flown soon after ex-Tropical Cyclone Gita. The highly erodible Separation Point Granite continues north into the Abel Tasman National Park. We would have expected the landslide distribution to also continue further north into Abel Tasman National Park, but this was not the case. Some possible reasons for this are discussed below. In addition to the high intensity rainfall, the surface geology appears to have been a critical factor controlling landslide initiation, with 80 % of the landslides occurring in Separation Point Granite (Figure 4.6 and Table 4.4), which occupies only 22.8 % of the area within the 130 mm rainfall contour, indicating that the geology was a major factor influencing where the landslides occurred.

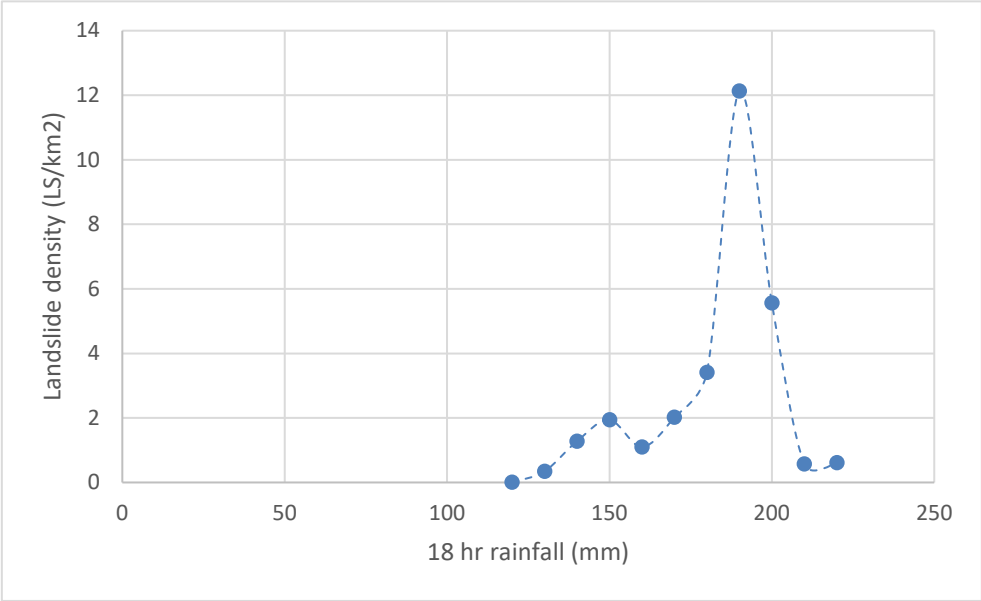


Figure 4.5 Relationship between landslide density and storm rainfall.

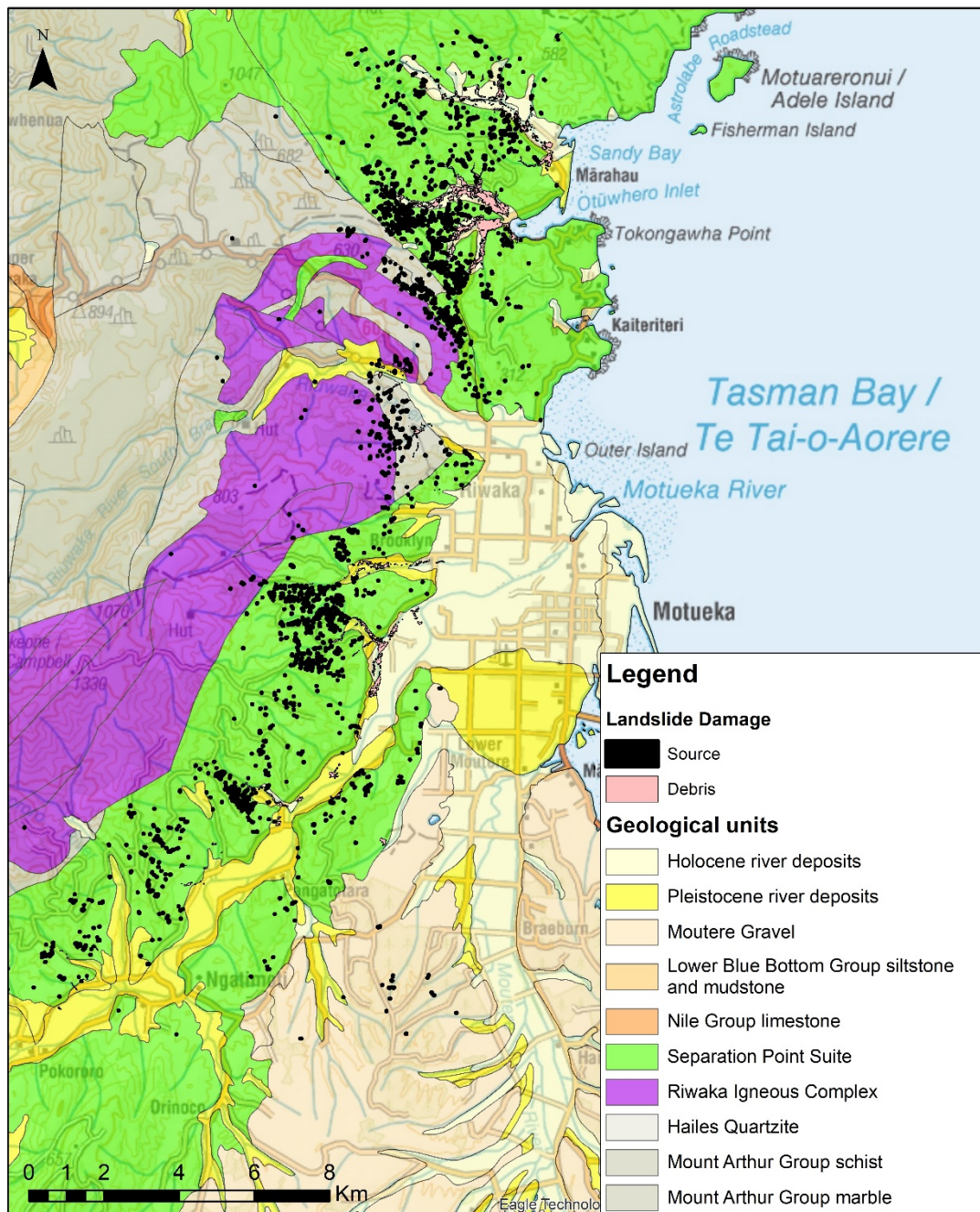


Figure 4.6 Landslide source area locations shown in relation to the underlying geology (after Heron 2018). Separation Point Granite is highlighted in green.

The frequency of landslides occurring in each of the slope categories is shown in Table 4.5. The majority of landslides occurred on slopes between 25 and 35 degrees. Landslides predominantly occurred on north-east facing slopes, with 72 % of landslides occurring on slopes with an aspect between 030 and 150 degrees (NNE to SE).

The distribution of landslides triggered by ex-Tropical Cyclone Gita in relation to main vegetation and land use classes (as mapped in 2012) in the Marahau-Riwaka area is shown in Figure 4.7 and the frequency of landslides occurring in each of the land use categories is shown in Table 4.6. The highest landslide densities were recorded on slopes with land use of scrub and exotic forestry. A third of the landslides (32.1 %) initiated on slopes with exotic forest land use, which only occupied 2 % of the area where rainfall was >130 mm. It is important to consider, however, that the exotic forest is planted on slopes underlain by the deeply

weathered Separation Point Granite. 63% of the area of Separation Point Granite is planted in exotic forestry.

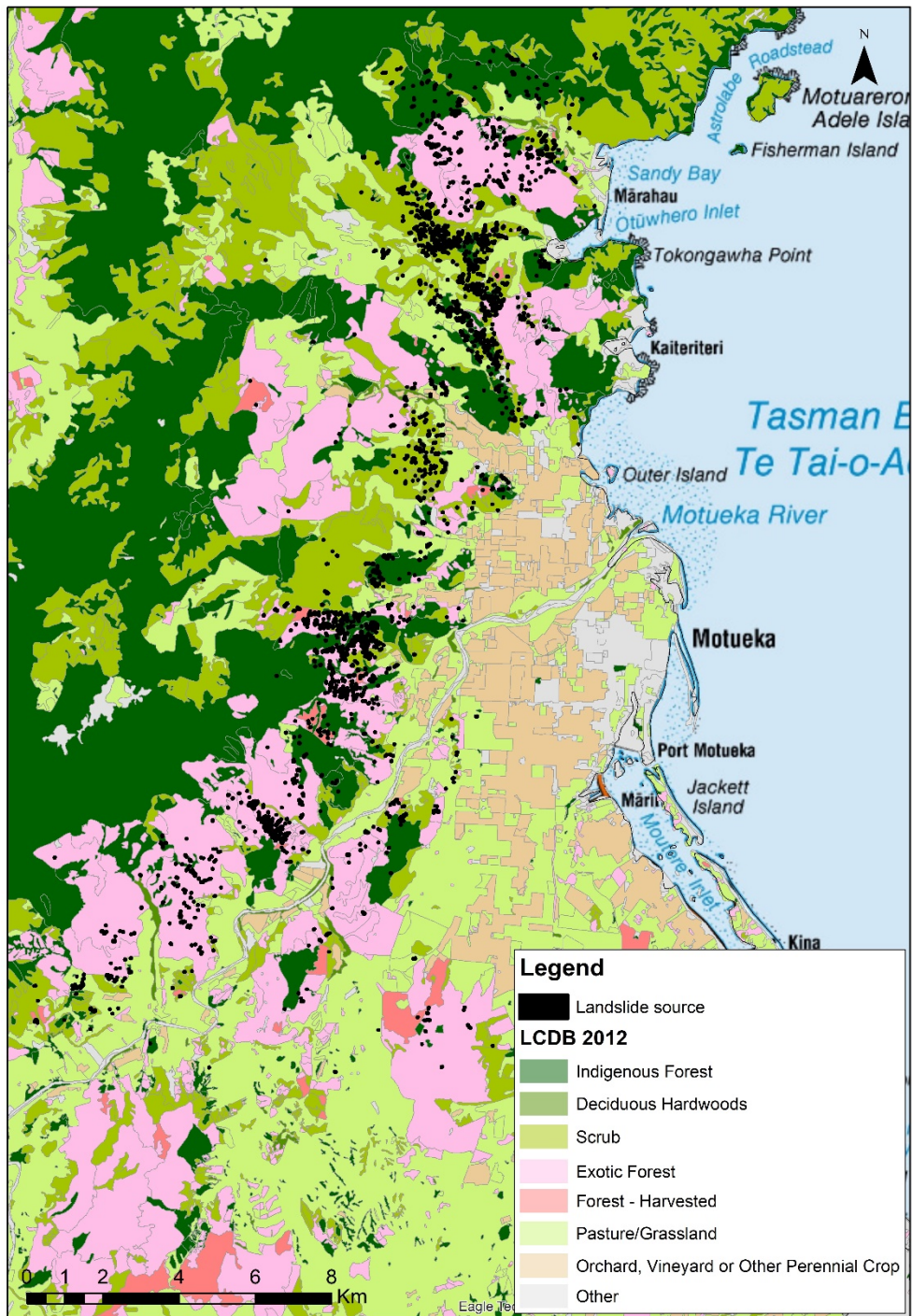


Figure 4.7 The distribution of landslides triggered by ex-Tropical Cyclone Gita in relation to main vegetation and land use classes (as mapped in 2012) in the Marahau-Riwaka area.

Table 4.4 Percentage (by number) of landslides (LS) triggered in each of the main geological units in the Marahau-Riwaka area.

Geology underlying landslide source areas	Number of landslides	%	% of area >130 mm	LS/km ²
Separation Point Granite	1354	80.0	22.8	2.9
Mount Arthur Group (marble, schist)	131	7.7	6.0	1.1
Riwaka Igneous Complex (diorite, gabbro)	111	6.6	4.4	1.2
Moutere Gravel (Tadmor Group)	18	1.1	25.6	0.0
Pleistocene alluvium	35	2.1	3.4	0.5
Holocene alluvium (river and fan deposits)	44	2.6	6.0	0.4
Other	0	0	31.8	0.0
Total	1639	100	100	

Table 4.5 The frequency of landslides occurring in each of the slope categories.

Maximum slope	Number of landslides	%	% of area affected	LS/km ²
<25	576	35.2	51.6	12.5
25-35	720	44.0	20.9	15.7
35-45	329	20.1	18.1	12.4
45-60	11	0.7	9.5	5.3
>60	0	0	0	0
Total	1636	100	100	

Table 4.6 The frequency of landslides occurring in the main land use categories (from LCDB2, mapped in 2012).

Land Use category (LCDB2)	Number of landslides	%	% area >130 mm rainfall	LS/km ²
Scrub (Fernland, Gorse and/or Broom, Manuka and/or Kanuka)	548	33.5	2.4	3.4
Indigenous forest	365	23.3	90.2	0.1
Exotic Forest	525	32.1	1.7	4.7
Forest - Harvested	37	2.3	0.2	2.6
Pasture	148	9.0	4.5	0.5
Deciduous Hardwoods	8	0.5	0.0	3.0
Orchard, Vineyard or other Crop	2	0.1	0.6	0.1
Other	3	0.2	0.4	0.1
Total	1636	100	100	

4.3 Melton Ratios

Melton Ratios were calculated for the 58 affected catchments in the Marahau area. Catchment characteristics and Melton Ratios (R) for these catchments are listed in Appendix 1. A scatterplot of Melton Ratio against catchment length is shown in Figure 4.8.

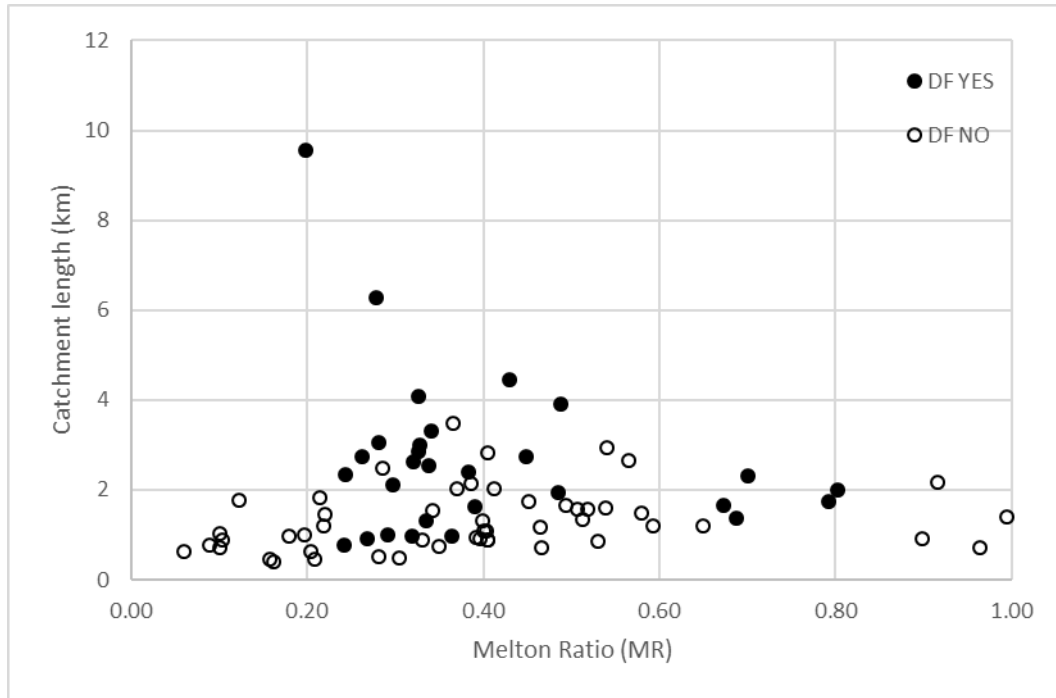


Figure 4.8 Melton Ratio and catchment length for the 58 affected catchments in the Marahau area. Catchments were classified according to debris flood/flow occurrence in ex-Tropical Cyclone Gita. The dashed line shows MR=0.3, above which catchments are thought to be capable of generating debris floods or debris flows.

The size of the catchment contributing area (upstream of the fan apex) for catchments that generated debris flows ranges from 0.4 to 26.3 km², and the catchment lengths (upstream of the fan apex) range from 0.8 to 9.5 km. Melton Ratios for catchments that generated debris flows range from 0.2 to 0.8. It is expected that catchments with a Melton Ratio >0.3 are capable of generating debris floods, and those with a Melton Ratio of >0.5 are capable of generating debris flows (Welsh & Davies 2011). We were not able to differentiate between debris floods and flows using the aerial photography alone.

5.0 DISCUSSION

Ex-Tropical Cyclone Gita reached New Zealand on 20–21 February 2018 bringing heavy rain and high winds across the country. Whilst its impacts were experienced nationally, the Nelson-Tasman region suffered some of the heaviest rainfall during the storm, which resulted in numerous landslides and, as a consequence, a local State of Emergency was declared in the Tasman region.

Following the storm GNS staff conducted a GeoNet landslide response, which comprised an aerial reconnaissance over the impacted areas and a rapid regional-scale landslide assessment using pre- and post-event satellite imagery differencing. The mapping identified approximately 2055 landslides that occurred during ex-Tropical Cyclone Gita, which were located in two areas:

- 1638 landslides were mapped in the Marahau-Riwaka area, over an area of about 130 km² (density of 12.6 landslides/km²).
- 417 landslides were mapped in the Aorere-Kaituna area of the Kahurangi National Park, over an area of about 38 km² (density of 11 landslides/km²).

Gauge-corrected rain radar data, recorded at the Wellington radar station, was supplied by MetService. We overlaid the landslide distribution derived from satellite imagery differencing onto the rain radar data for the 18-hour (storm total) maximum and there were two inconsistencies that showed up. Firstly, in the Marahau-Riwaka area, analysis showed that the maximum landslide density occurred in the areas that received 190–200 mm of rainfall near the Marahau River, although higher rainfall was recorded north of this in Abel Tasman National Park (235 mm). Secondly, the distribution of landslides in the Aorere-Kaituna river area indicated a much lower rainfall threshold (~86 mm/24 hrs) which was unlikely to have triggered slope failure, especially on slopes in indigenous forest. Both of these inconsistencies are likely to be related to the distance of the rain radar station (Wellington) from the study area.

Due to the distance from the MetService Wellington radar station (approx. 145 km) and the curvature of the earth, the Wellington rain radar estimated the rainfall over the Marahau area at an altitude of about 3 km above mean sea level (a.m.s.l). During the period of heaviest rainfall (3 pm to 6 pm on 20 February), the wind at 3 km altitude over Marahau was a very strong northerly of 60–70 knots (110–130 km/hr), decreasing to an easterly wind of 35–40 knots (65–75 km/hr) near the ground surface. These data were obtained from a MetService 8 km resolution weather model. Due to the very strong northerly winds during the period of heaviest rainfall, it is estimated that the radar-derived rainfall at 3 km height over the Marahau area probably reached the ground about 10 km further south than indicated on the radar rainfall map. There are no rain gauges in this area (Figure 1.2) with which to correct the radar data. Shifting the rain radar data 10 km south would align the maximum rainfall with the maximum observed landslide density, and the catchments that experienced the biggest debris flows (Otuwhero and Marahau Rivers).

For the Aorere-Kaituna area, the distance to the Wellington radar station is approximately 180 km. The same limitations apply as for the Marahau-Riwaka area, with the rainfall being measured at a height of about 4.1 km, which was about the height of the freezing level during this event, which means that the radar was measuring melting snow and ice. A significant amount of rain may also have formed below this height which suggests the radar may have underestimated rainfall in this location. Because the Aorere-Kaituna area was effectively masked by the heavy rainfall in the Riwaka-Marahau area (in direct line-of-sight from Wellington), any attenuation occurring from the heavy rain over Abel Tasman would have

made the estimates worse. Additionally, MetService did not have access to the TDC ‘Devils Boot’ rain gauge, which may have improved radar-derived rainfall estimates.

Because – at least in this case – the rain radar data does not reflect where the rain actually fell on the ground surface, analysis of rainfall triggering thresholds for debris flows was not attempted. However, visual interpretation suggests that the threshold for triggering debris flows in Separation Point Granite was about 200 mm/18hrs, and 120 mm/3 hrs. This equates to rainfall intensities >10 mm/hr for an extended period of time or 40 mm/hr for 3 hours. This is similar to the rainfall intensities reported by Page et al. (2012) for the December 2011 Ligar Bay debris flows, that were triggered by 395 mm of rain in 24 hrs, or an average rainfall intensity of 16 mm/hr for 24 hrs, and Basher (2010) who reported that debris flows at Tapawera (also underlain by Separation Point Granite) in 2010 were triggered by short duration rainfall intensities of 40-70 mm/hr. Recent debris flow events in the Tasman District are summarised in Table 5.1.

Table 5.1 Previous storm events that have triggered debris flows in the Tasman District.

Storm dates	Rainfall data	Main geological unit impacted	Impacts
16/05/2010	Approximately 200 mm during event Max intensity 40–70 mm/hr	Separation Point Granite	Landslides and debris flows in lower Wangapeka and Baton River catchments (Basher 2010)
13–15/12 2011	674 mm recorded in 48 hrs 454 mm in 24 hrs	Separation Point Granite	Several landslides in hills east of Takaka; Several Properties situated on debris fans destroyed by debris flows on in Pohara Valley and Nyhane Drive in Ligar Bay area (Page et al. 2012)
21/04/2013	127 mm in 2 hrs	Riwaka Complex Gabbro	Fatal debris flow in Riwaka Valley (Page 2013)
15–17/06/2013	168 mm in 24 hrs	Separation Point Granite	Fatal debris flow at Otuwhero Inlet (Page 2013)
24/3/2016	304 mm in 24 hrs	Separation Point Granite	Major flooding and landslides at Takaka

Page et al. (2012) found evidence for several other debris flow events in the Ligar Bay area and suggested a rainfall return period of 200+ years for debris flows in the Tasman region on Separation Point Granite. The return period for the 1, 3 and 12-hour rainfall totals in ex-Tropical Cyclone Gita also likely exceed 200 years at Marahau and the Abel Tasman National Park, adding further weight to the conclusion that a rainfall return period of 200+ years is required to trigger debris flows on highly weathered areas of Separation Point Granite.

In this study we used differencing of pre- and post-event 10 m resolution Sentinel satellite imagery to map the landslide distribution. Although differencing of Sentinel imagery was good at detecting strong spectral differences between pre- and post-event imagery, and therefore determining the locations of new landslides, the resolution of the imagery limited its usefulness to produce a reliable detailed landslide inventory. The average size of landslides (source + deposit) in the Marahau-Riwaka area was 783 m², which is roughly 8 pixels, so there was not enough detail to differentiate between landslide source area and deposit. Landslides that

coalesce to form a single deposit were also not able to be differentiated. The resolution of the imagery also limited our ability to differentiate between bank erosion and stream-side landslides, or overbank deposition on the adjacent floodplain. Additionally, many small landslides (100–300 m²) were not detected. Many of the areas where landslides occurred in the Marahau-Riwaka area were also affected by storms in December 2011 (Page et al. 2012), June 2013 (Page 2013), March and May 2016, and April 2017 (Cyclone Debbie) so there were many places where there were existing landslides. In these areas, differencing of Sentinel imagery was not very good at picking up new landslides in close proximity to existing landslides, nor enlargement or reactivation of existing landslides (Figure 5.1). An assessment of the accuracy of 3 and 10 m resolution satellite imagery differencing for detecting new landslides found that the errors and misclassifications are potentially significant, particularly in recently deforested areas, and that landslide distributions should be checked against suitable high-resolution satellite imagery or aerial photography (Rosser et al. 2019).

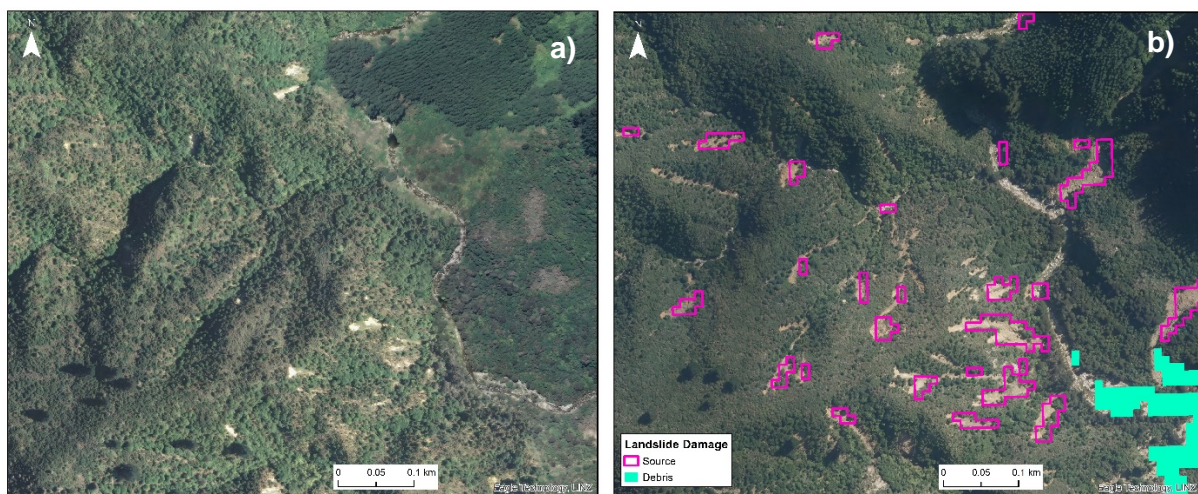


Figure 5.1 Aerial photographs of landslides in The Shaggy catchment taken a) before (2016) and b) after ex-Tropical Cyclone Gita (March 2018), showing the landslide polygons derived from Sentinel imagery differencing. There are several existing landslides evident in the pre-storm imagery. Differencing was not able to detect many of the observed new landslides or enlargement of existing landslides. It was also not able to differentiate landslide sources areas from deposits or landslides with coalescing deposits. Aerial photos (0.3 m resolution) were provided by TDC.

Although differencing of 10 m-resolution Sentinel imagery was not able to provide detailed mapping of landslides at a scale that would provide morphological information about the landslides (areas of source and deposit), it did provide a very quick assessment of the likely locations of new landslides, and an assessment of the number and scale of landsliding triggered by the storm event. It also permitted rapid mapping of the extent of deposition from both overbank flooding and debris flows, although it was difficult to differentiate the two without the use of high-resolution aerial photography.

The landslide distribution was also analysed in relation to the geology, vegetation/landuse, slope angle and aspect characteristics of each landslide source area. In the Marahau-Riwaka region the surface geology appears to have been a critical control on the landslide distribution with 80 % of the landslides occurring on Separation Point Granite which underlies only 23 % of the affected land area. The Separation Point Granite suite is commonly deeply weathered and highly erodible and is well known for its erosion problems (Basher et al. 2003). The underlying geology seems to be less important in the Aorere-Kaituna area, with no observed correlation between landslide occurrence and geological substrate. There were equal numbers of landslides on Anatoki Formation sandstone and Waingarō schist.

Vegetation or land cover also had a strong influence on the distribution of landslides, particularly in areas underlain by Separation Point Granite. In the Marahau-Riwaka area, the highest landslide densities were recorded on exotic forest, scrub and harvested forestry areas. A third of the landslides (32.8 %) were triggered on slopes with exotic forest land use which only occupied 2 % of the area where rainfall was >130 mm (based on the rain radar data). Exotic forest (as mapped in 2012) included considerable areas of new plantings and areas that have been logged since 2012, but no data on these areas was available for this report. Observations from the reconnaissance flight and the aerial photography suggest many of the landslides were located in areas of recent logging or new forest planting, and many were associated with forest roads and skid platforms. In the Tapawera 2010 storm event, Basher (2010) reported that landslides (debris flows) occurred on slopes in plantation forests, much of which had been recently harvested. Landslides were most common on recently clear-felled slopes (<2-5 yrs) but were also common in mature pine trees with extensive windthrow in canopy gaps. It is important to remember that the exotic forest was planted on slopes underlain by the highly erodible Separation Point Granite for erosion control (and partly because of infertile soils) (Basher et al. 2003), and a large proportion (63 %) of the area of Separation Point Granite is planted in exotic forestry so these are not independent variables.

In the Aorere-Kaituna area, 90 % of the landslides triggered by ex-Tropical Cyclone Gita occurred on slopes with Indigenous forest, which covers about 82 % of the affected area. There, the threshold for triggering rainfall-induced landslides in indigenous forest was around 60 mm in 3 hours, a return period of about 50 yrs (HIRDS).

The majority of landslides occurred on north-east facing hillslopes with slopes between 25 and 35 degrees, with 72 % of landslides occurring on slopes facing NNE to SE. The storm approached from the northeast, so northeast facing slopes received more rain.

Unlike the debris flow catchments studied by Page et al. 2012, there does not seem to be a clear difference in Melton Ratios (MR) between catchments that did or didn't generate debris flows in ex-Tropical Cyclone Gita (Figure 4.7). Catchment lengths (upstream of fan apex) were greater than 0.8 km, similar to Page et al. (2012), however Melton Ratios as low as 0.2 were calculated for catchments that produced debris floods and flows in ex-Tropical Cyclone Gita. We were not able to differentiate between debris floods and flows in this study. One possible reason for this is that the highest rainfall was concentrated in the lower part of many of the larger catchments in which debris flows occurred (see Figure 3.3). Debris floods and flows were generated by landslides that only occurred in the lower reaches of the rivers, so the whole contributing catchment area and length was not contributing to the debris flow generation in this case. This means that debris flows were generated in catchments with lower Melton Ratios than expected (MR <0.3) because larger catchments also generated debris flows in their lower reaches rather than just short steep catchments. There were also catchments with a Melton Ratio of >0.3 and similar rainfall characteristics that did not produce debris flows. Melton Ratios do not consider the rainfall that triggered the debris flows. The rainfall characteristics may have had a greater influence over where debris flows were triggered in ex-Tropical Cyclone Gita.

6.0 CONCLUSIONS

- Ex-Tropical Cyclone Gita hit the Tasman District in February 2018, bringing with it extreme rainfall. The highest rainfall was recorded in the Marahau-Riwaka area, where 235 mm fell in 18 hours, with maximum intensities of 75 mm/hr. The estimated return period for this rainfall was 200+ years.
- Landslides were mapped by a semi-automated classification using differencing of pre- and post-event 10 m resolution Sentinel satellite imagery. While differencing did provide a very quick assessment of the likely locations of new landslides, and an assessment of the number and scale of landslides and deposition during the storm, the resolution of the imagery did not permit detailed mapping of landslide morphology such as differentiating landslide source area from deposit, coalescing landslides or differentiating stream-side landslides and bank erosion from overbank deposition.
- The extreme rainfall triggered more than 2000 landslides, in two distinct areas. Approximately 1638 landslides were observed in the Riwaka-Marahau area, and 417 in the Aorere-Kaituna area of Kahurangi National Park. Debris flows were initiated in several of the receiving catchments, particularly in the Riwaka-Marahau area, where significant debris flows occurred in the Otuwhero, Marahau, Riwaka, Rocky and the Shaggery rivers.
- The majority of landslides triggered by the storm were shallow soil slip and debris flows in soil or colluvium, predominantly initiated in gully heads, although there were some deeper-seated landslides and rockfalls.
- In the Riwaka-Marahau area, the distribution of landslides was strongly influenced by the underlying geology, with 80% of the landslides occurring on Separation Point Granite which underlies only 23% of the area where landslides occurred. Rocks of the Separation Point Granite suite are often deeply weathered and highly erodible (Basher et al. 2003). In the Aorere-Kaituna area, geology was less important, with approximately equal landslide numbers occurring in Anatoki Formation sandstone and Waingaro schist.
- The rainfall threshold for triggering debris flows in Separation Point Granite was about 200 mm/18 hrs, or 120 mm/3 hrs. This equates to rainfall intensities >10 mm/hr for longer durations (24 hrs) or 40 mm/hr for shorter durations (~3 hours), which agrees with other studies of landslides and debris flows on Separation Point Granite in the Tasman District (Page et al. 2012; Basher 2010).
- Vegetation or land cover also had a strong influence on the distribution of landslides, particularly in areas underlain by Separation Point Granite that had been recently harvested. In the Marahau-Riwaka area, the highest landslide densities were recorded on exotic forest, scrub and harvested forestry areas. Observations from the aerial reconnaissance and photography suggest that areas of recent logging, forest roads and skid platforms experienced higher landslide densities. Most of the developed areas of Separation Point Granite are planted with exotic forest, in part to help prevent landslides and erosion.

- Analysis of the landslide distribution in relation to the rainfall estimates derived from MetService rain radar identified several issues, mostly associated with the distance from the Wellington radar station. Firstly, due to the distance from the radar, the rainfall was measured at a height of 3–4 km. With northerly winds of 110–130 km/hr, it was estimated that the rain fell on the ground roughly 10 km south of where it was measured in the air. Secondly, the radar had difficulty ‘seeing through’ the heavy rain at Abel Tasman National Park and underestimated the rainfall in the Kahurangi National Park. Ideally, when using rain radar to investigate rainfall induced landslides, it should be corrected for wind, and used with caution.

7.0 ACKNOWLEDGMENTS

Funding for this project was provided through GeoNet. Tasman District Council provided pre- and post-event aerial photography and rainfall data. The authors gratefully acknowledge the reviews provided by Mike Page and Saskia de Vilder.

8.0 REFERENCES

- Basher LR, compiler. 2003. The Motueka and Riwaka catchments: a technical report summarising the present state of knowledge of the catchments, management issues and research needs for integrated catchment management. Lincoln (NZ): Landcare Research. 119 p.
- Basher LR. 2010. Storm damage in the Tapawera area during the storm of 16 May 2010 [unpublished report]. [Lincoln (NZ)]: Landcare Research. 17 p.
- Coker RJ, Fahey BD. 1993. Road-related mass movement in weathered granite, Golden Downs and Motueka Forests, New Zealand: a note. *Journal of Hydrology (New Zealand)*. 31(1):65-69.
- Coker RJ, Fahey BD. 1994. Separation Point granite terrain erosion and sedimentation risk. [Lincoln (NZ)]: Landcare Research. Contract Report LC9394/70. Prepared for Tasman District Council.
- Fahey BD, Coker RJ. 1989. Forest road erosion in the granite terrain of Southwest Nelson, New Zealand. *Journal of Hydrology (New Zealand)*. 28(2):123-141.
- Heron DW, custodian. 2018. Geological map of New Zealand 1:250,000. 2nd ed. Lower Hutt (NZ): GNS Science. 1 CD. (GNS Science geological map; 1).
- Hungr O, McDougall S, Bovis M. 2005. Entrainment of material by debris flows. In: Jakob M, Hungr O, editors. *Debris-flow Hazards and Related Phenomena*. Berlin (DE): Springer. p. 135–158.
- Hungr O, Leroueil S, Picarelli L. 2014. The Varnes classification of landslide types, an update. *Landslides*. 11(2):167–194. doi:10.1007/s10346-013-0436-y.
- Page MJ, Langridge RM, Stevens GJ, Jones KE. 2012. The December 2011 debris flows in the Pohara-Ligar Bay area, Golden Bay: causes, distribution, future risks and mitigation options. Lower Hutt (NZ): GNS Science. 91 p. Consultancy Report 2012/305. Prepared for Tasman District Council.
- Page MJ. 2013. Landslides and debris flows caused by the 15-17 June 2013 rain storm in the Marahau-Motueka area, and the fatal landslide at Otuwhero Inlet. Lower Hutt (NZ): GNS Science. 35 p. (GNS Science report; 2013/44).
- Rattenbury MS, Cooper RA, Johnston MR, compilers. 1998. Geology of the Nelson area [map]. Lower Hutt (NZ): GNS Science. 1 folded map + 67 p., scale 1:250,000. (Institute of Geological & Nuclear Sciences 1:250,000 geological map; 9).
- Rosser BJ, Ashraf S, Dellow GD. 2019. Assessment of the use of differencing satellite imagery as a tool for quantifying landslide impacts from significant storms – a case study in the Uawa catchment, Tolaga Bay. Lower Hutt (NZ): GNS Science. 51 p. Consultancy Report 2019/93. Prepared for Gisborne District Council
- Rosser BJ, Dellow GD, Massey CI. [2020]. Rainfall intensity–duration thresholds for shallow landslides in New Zealand (in review).
- van de Graaf M, Wagtendonk A. 1991. Road-related mass wasting, Golden Downs and Motueka Forests, south-west Nelson, New Zealand. [unpublished report]. Christchurch (NZ): Forest Research Institute.
- Welsh A, Davies T. 2011. Identification of alluvial fans susceptible to debris-flow hazards. *Landslides*. 8:183–194. doi:10.1007/s10346-010-0238-4.

APPENDICES

This page left intentionally blank.

APPENDIX 1 CATCHMENT CHARACTERISTICS AND MELTON RATIOS

Catchment ID	Name	Debris flood/flow	Drainage length (km)	Relief (m)	Catchment area (km ²)	Melton Ratio
Marahau_0	Brooklyn1	Yes	3039.1	440.2	2.5	0.28
Marahau_1	Brooklyn3	Yes	4442.0	937.2	4.7	0.43
Marahau_2	Brooklyn4	Yes	3899.9	753.9	2.4	0.49
Marahau_3	Otuwhero4	Yes	9554.7	1018.2	26.3	0.20
Marahau_4	Marahau1	Yes	4079.2	1000.2	9.4	0.33
Marahau_5	Pangatotara	Yes	3297.6	889.3	6.8	0.34
Marahau_6	Brooklyn5	Yes	6277.0	1018.7	13.3	0.28
Marahau_7	Otowhero1	Yes	2724.5	993.2	14.3	0.26
Marahau_8	Marahau2	Yes	2621.7	694.0	4.7	0.32
Marahau_9	Otuwhero	Yes	2391.8	694.0	3.3	0.38
Marahau_10	Otuwhero2	Yes	2724.5	694.0	2.4	0.45
Marahau_11	Riwaka	Yes	2996.8	625.4	3.6	0.33
Marahau_12	Sandy Bay	Yes	910.3	180.5	0.5	0.27
Marahau_22		No	2927.9	815.2	2.3	0.54
Marahau_23		No	1012.5	104.9	1.1	0.10
Marahau_24		No	465.8	68.4	0.2	0.16
Marahau_25		No	2845.1	756.2	5.4	0.33
Marahau_26		Yes	2545.0	449.6	1.8	0.34
Marahau_27		No	1777.8	122.3	1.0	0.12
Marahau_28		No	3475.6	679.6	3.5	0.37
Marahau_29		No	504.7	148.1	0.3	0.28
Marahau_30		No	1826.8	292.6	1.9	0.21
Marahau_31		No	714.7	82.5	0.7	0.10
Marahau_32		No	2491.7	412.2	2.1	0.29
Marahau_33		No	960.6	131.4	0.5	0.18
Marahau_34		No	1010.7	221.3	0.6	0.29
Marahau_35		Yes	957.5	245.0	0.5	0.36
Marahau_36		No	1580.8	496.0	0.9	0.52
Marahau_37		No	767.0	104.1	1.4	0.09
Marahau_38		No	875.1	70.2	0.5	0.10
Marahau_39		Yes	768.1	196.0	0.7	0.24
Marahau_40		No	385.0	205.7	1.6	0.16
Marahau_41		No	1310.9	337.1	1.0	0.33
Marahau_42		No	718.8	248.6	0.3	0.47
Marahau_43		No	1398.3	367.2	0.1	0.99

Catchment ID	Name	Debris flood/flow	Drainage length (km)	Relief (m)	Catchment area (km ²)	Melton Ratio
Marahau_44		No	1453.5	228.0	1.1	0.22
Marahau_45		No	2648.3	685.8	1.5	0.56
Marahau_46		No	1588.4	513.1	0.9	0.54
Marahau_47		No	631.3	147.1	0.5	0.20
Marahau_48		Yes	967.4	222.8	0.5	0.32
Marahau_49		No	1079.8	341.7	0.7	0.40
Marahau_50		Yes	1930.9	554.3	1.3	0.49
Marahau_51		No	446.8	117.9	0.3	0.21
Marahau_52		No	733.7	227.0	0.4	0.35
Marahau_53		No	872.0	220.3	0.3	0.41
Marahau_54		No	627.9	264.8	19.3	0.06
Marahau_55		No	983.5	143.0	0.5	0.20
Marahau_56		No	1192.6	367.9	0.3	0.65
Marahau_57		No	1165.9	331.9	0.5	0.46
Marahau_58		No	492.9	146.1	0.2	0.31
Marahau_59		No	1189.2	159.4	0.5	0.22
Marahau_60		No	890.6	140.0	0.2	0.33
Marahau_61		No	1095.7	263.7	0.4	0.40
Marahau_62		No	1202.4	355.5	0.4	0.59
Marahau_63		No	870.5	244.2	0.4	0.41
Marahau_64		No	858.9	328.2	0.4	0.53
Marahau_65		No	944.6	224.0	0.3	0.39
Marahau_66		No	1660.1	481.8	1.0	0.49



www.gns.cri.nz

Principal Location

1 Fairway Drive, Avalon
Lower Hutt 5010
PO Box 30368
Lower Hutt 5040
New Zealand
T +64-4-570 1444
F +64-4-570 4600

Other Locations

Dunedin Research Centre
764 Cumberland Street
Private Bag 1930
Dunedin 9054
New Zealand
T +64-3-477 4050
F +64-3-477 5232

Wairakei Research Centre
114 Karetoto Road
Private Bag 2000
Taupo 3352
New Zealand
T +64-7-374 8211
F +64-7-374 8199

National Isotope Centre
30 Gracefield Road
PO Box 30368
Lower Hutt 5040
New Zealand
T +64-4-570 1444
F +64-4-570 4657